

Photoluminescence Properties of Tetrahedral Zinc(II) Complexes

Supported by Calix[4]arene-based Salicylaldiminato Ligands

Steve Ullmann,^a René Schnorr,^a Christian Laube,^b Bernd Abel,^{*b,c} and Berthold Kersting^{a,*}

^a Institut für Anorganische Chemie, Universität Leipzig, Johannisallee 29, 04103 Leipzig, Germany, E-mail: b.kersting@uni-leipzig.de Fax: +49(0)341-97-36199

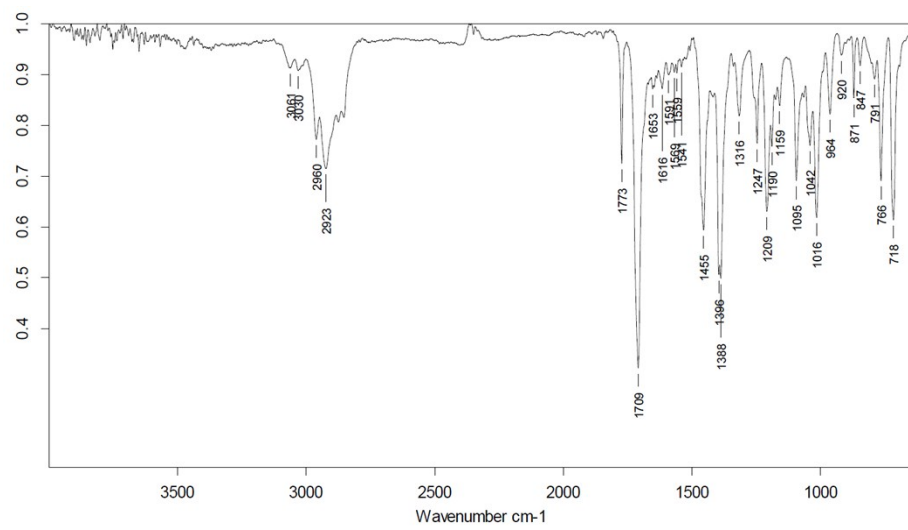
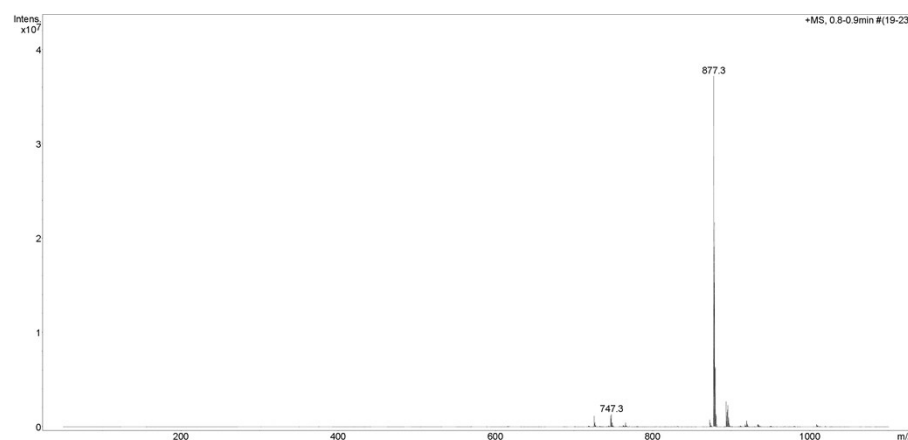
^b Leibniz-Institut für Oberflächenmodifizierung e. V., Chemische Abteilung, D-04318 Leipzig, Germany

^c Wilhelm-Ostwald-Institut für Physikalische und Theoretische Chemie, Universität Leipzig, Linnéstraße 2, D-04103 Leipzig, Germany

Keywords: Calixarenes / Salicylaldiminato Ligands / Tetrahedral Zinc Complex /

Photoluminescence

Supporting Information

1.) Analytical data for compound 4.**Figure S1.** Infrared spectrum of 4.**Figure S2.** ESI mass spectrum of 4.

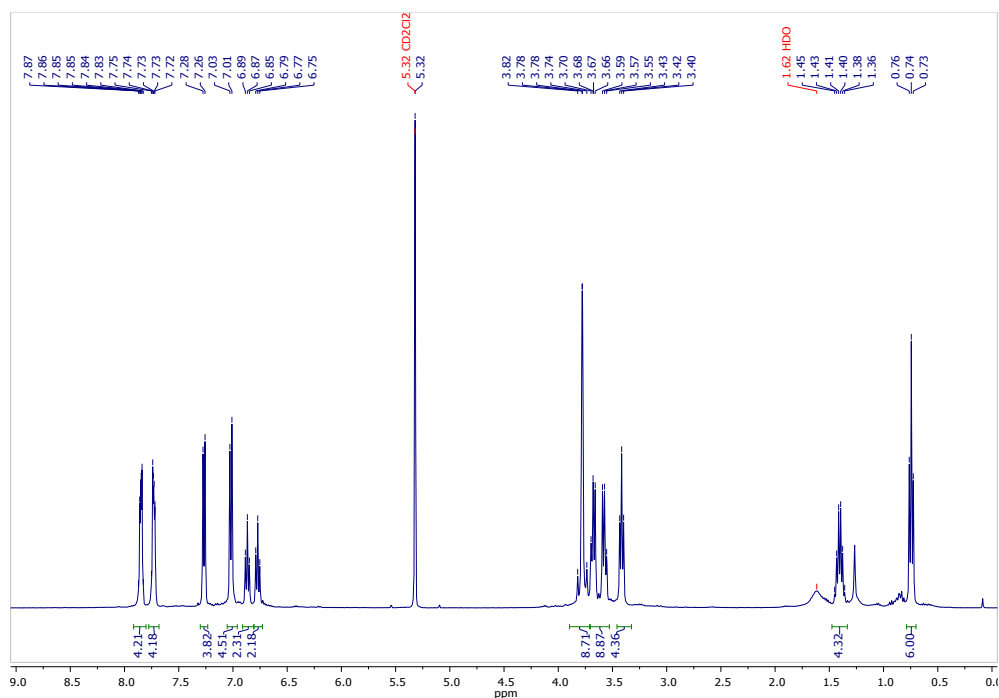


Figure S3. ^1H NMR spectrum of **4** in CD_2Cl_2 at ambient temperature.

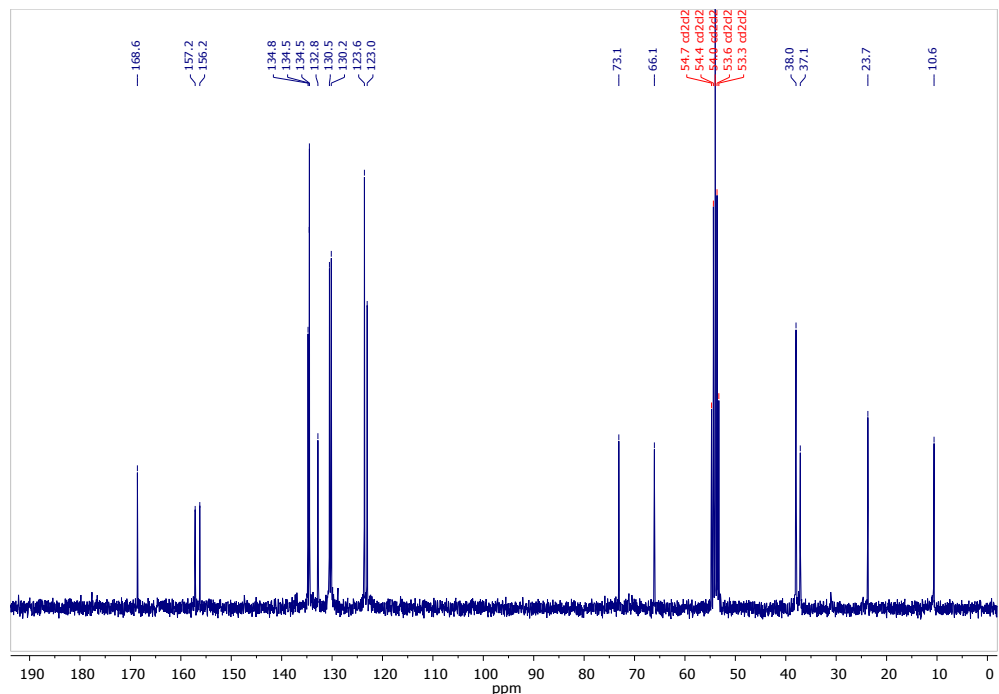


Figure S4. ^{13}C NMR spectrum of **4** in CD_2Cl_2 at ambient temperature.

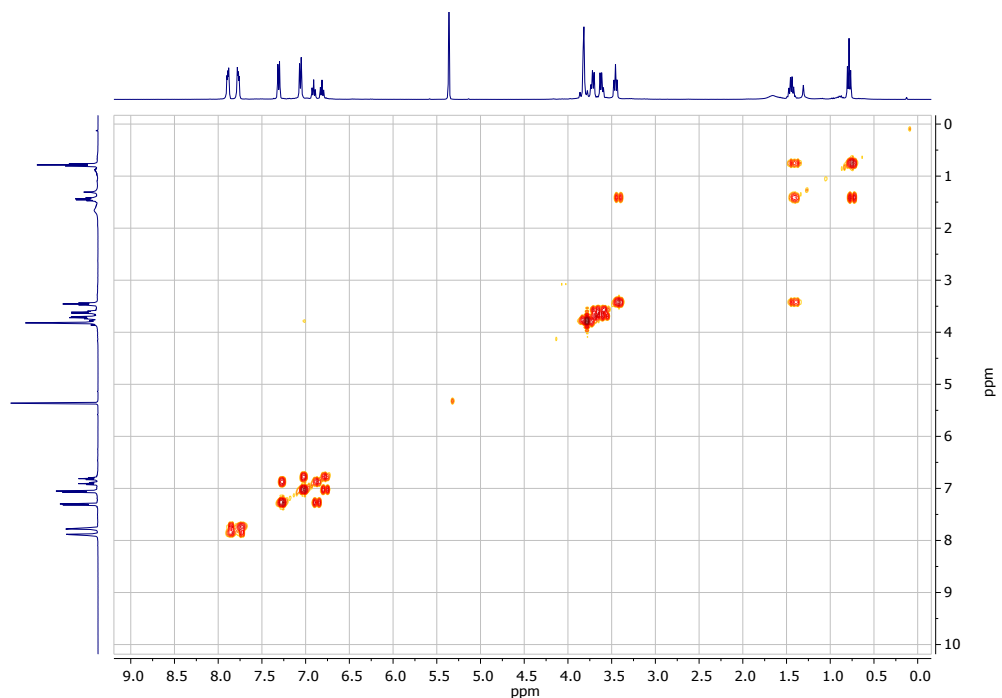


Figure S5. ¹H, ¹H COSY spectrum of **4** in CD₂Cl₂ at ambient temperature.

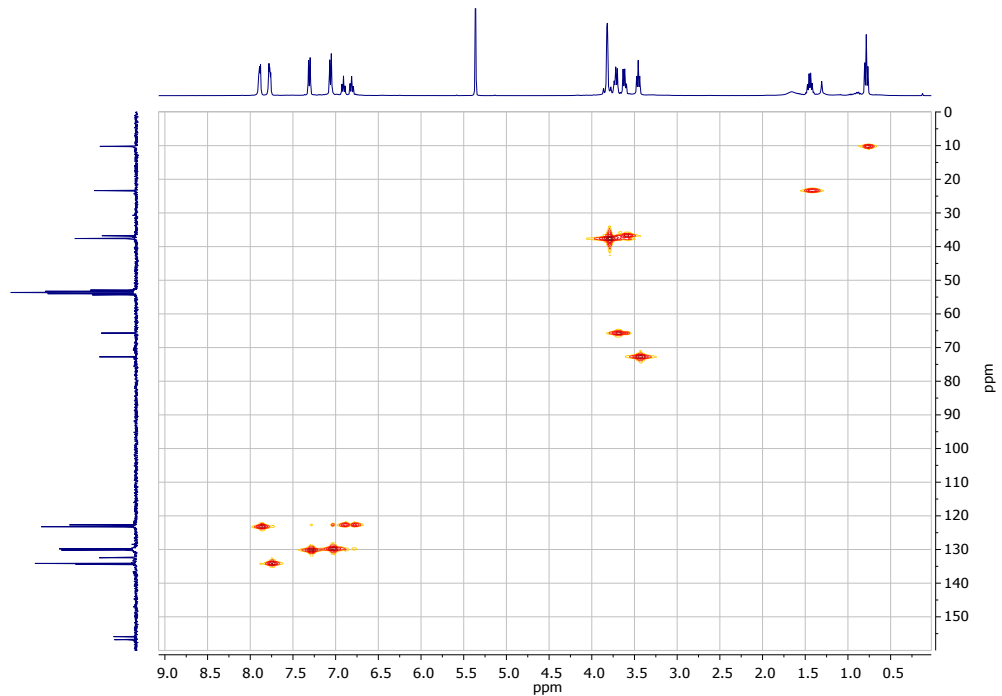


Figure S6. ¹H, ¹³C HSQC spectrum of **4** in CD₂Cl₂ at ambient temperature.

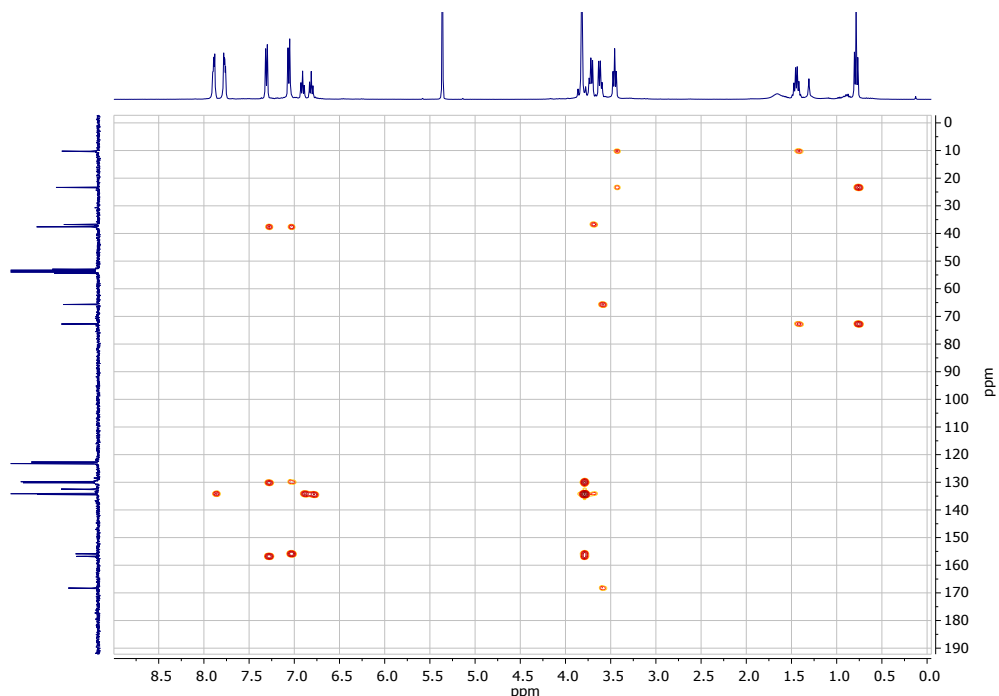


Figure S7. $^1\text{H}, ^{13}\text{C}$ HMBC spectrum of **4** in CD_2Cl_2 at ambient temperature.

1,3-alt 25,27-Di(phthalimidoethoxy)-26,28-di(n-propyloxy)-calix[4]aren (**4**)

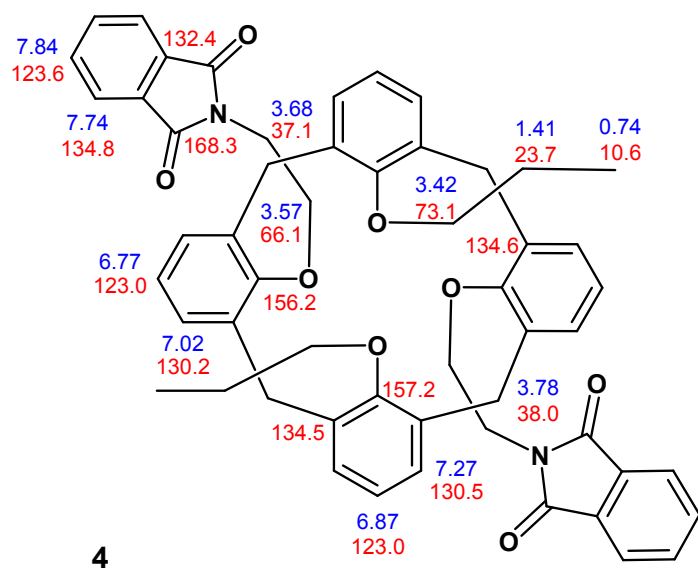


Figure S8. Assignment of NMR signals for **4** (blue: ^1H , red: ^{13}C)

2) Analytical data for Compound 5.

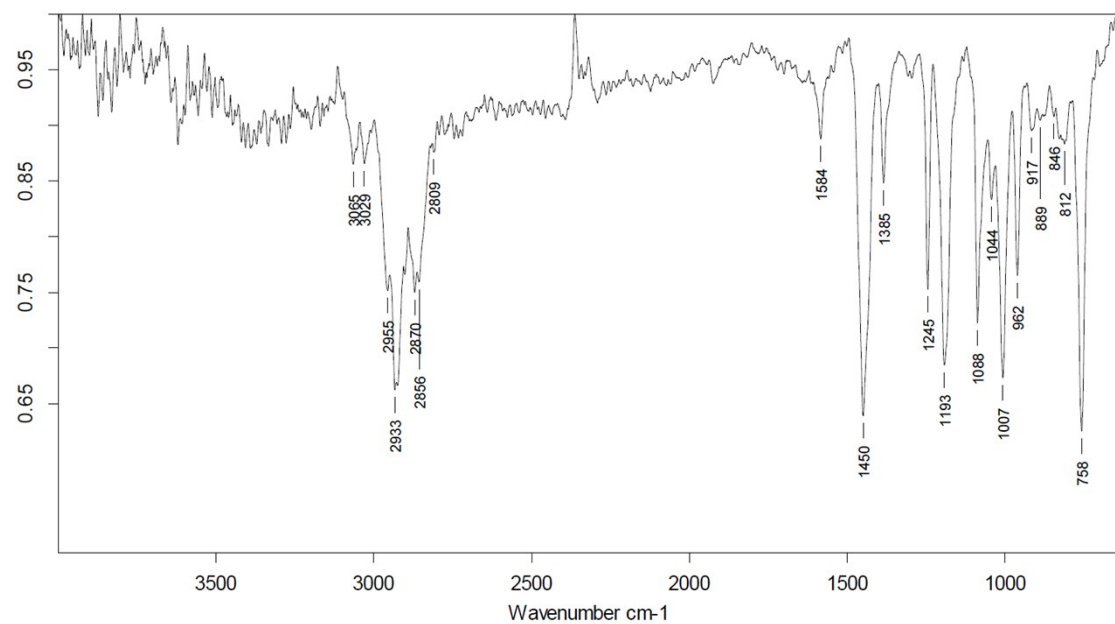


Figure S9. Infrared spectrum of **5**

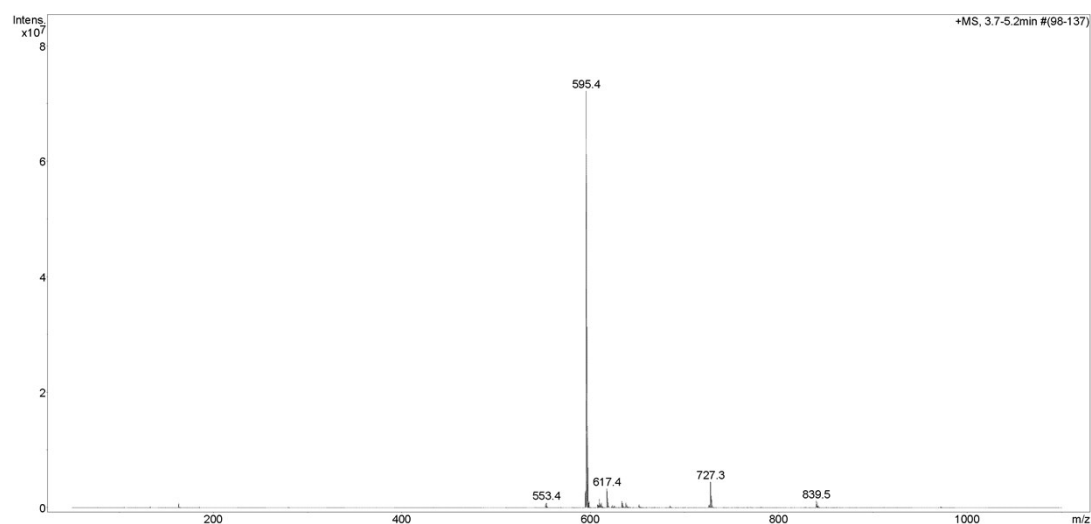


Figure S10. ESI mass spectrum of **5**.

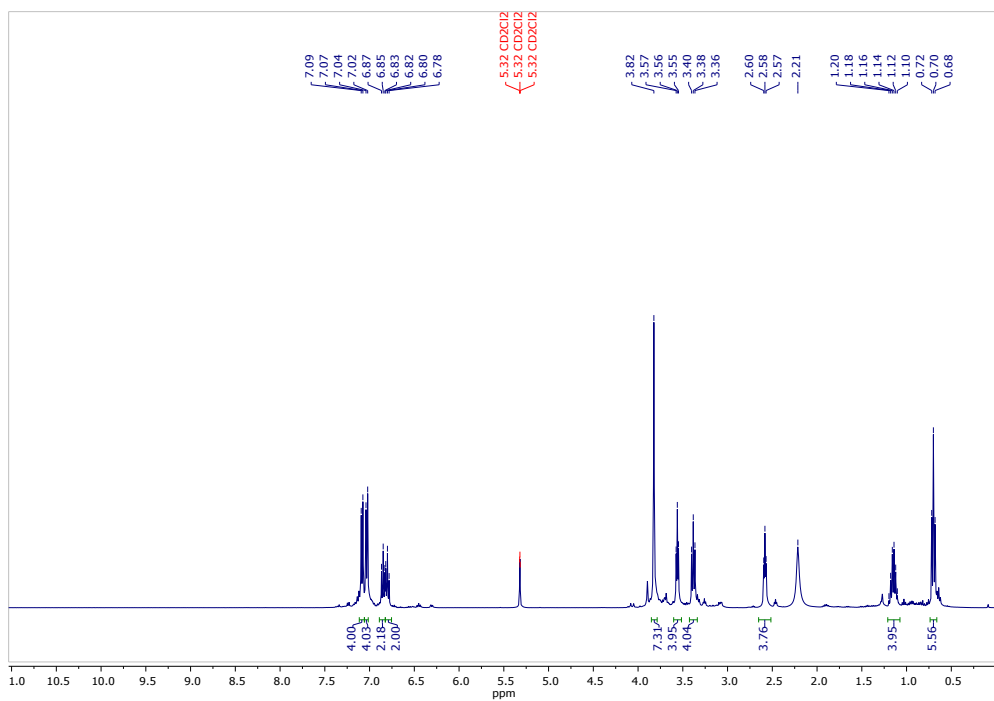


Figure S11. ¹H NMR spectrum of **5** in CD₂Cl₂ at ambient temperature.

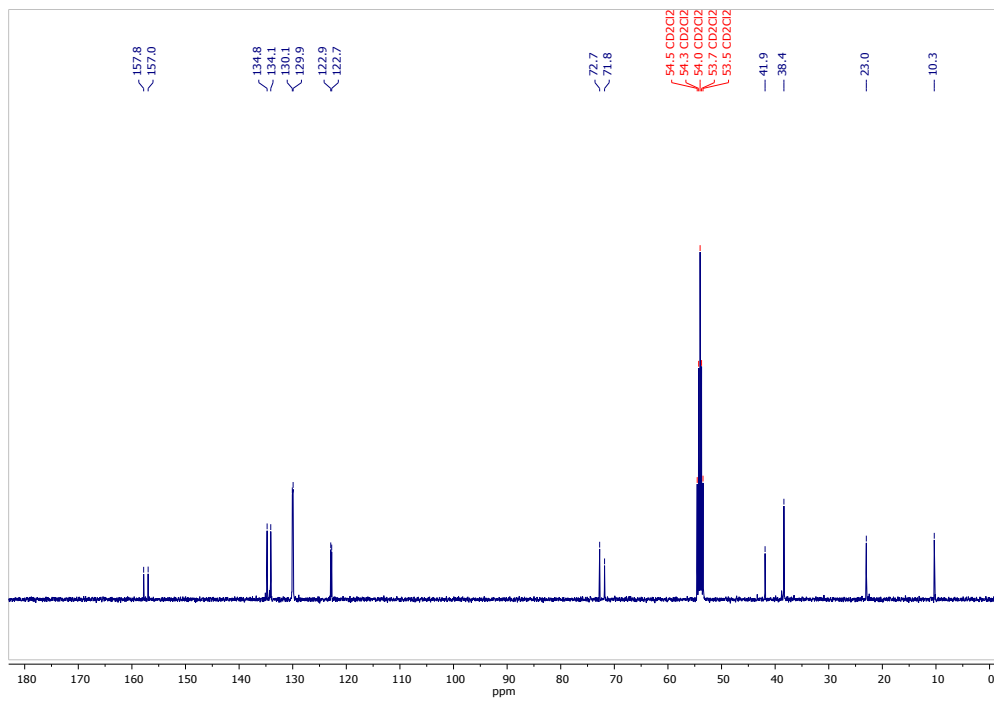


Figure S12. ¹³C NMR spectrum of **5** in CD₂Cl₂ at ambient temperature.

1,3-alt 25,27-Di(aminoethoxy)-26,28-di(n-propyloxy)-calix[4]aren (**5**)

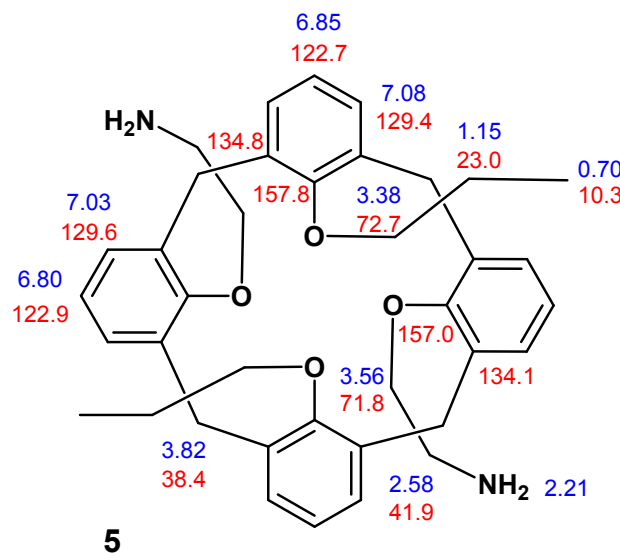


Figure S13. Assignment of NMR signals for **5** (blue: ^1H , red: ^{13}C)

3) Analytical data for compound H_2L^1 .

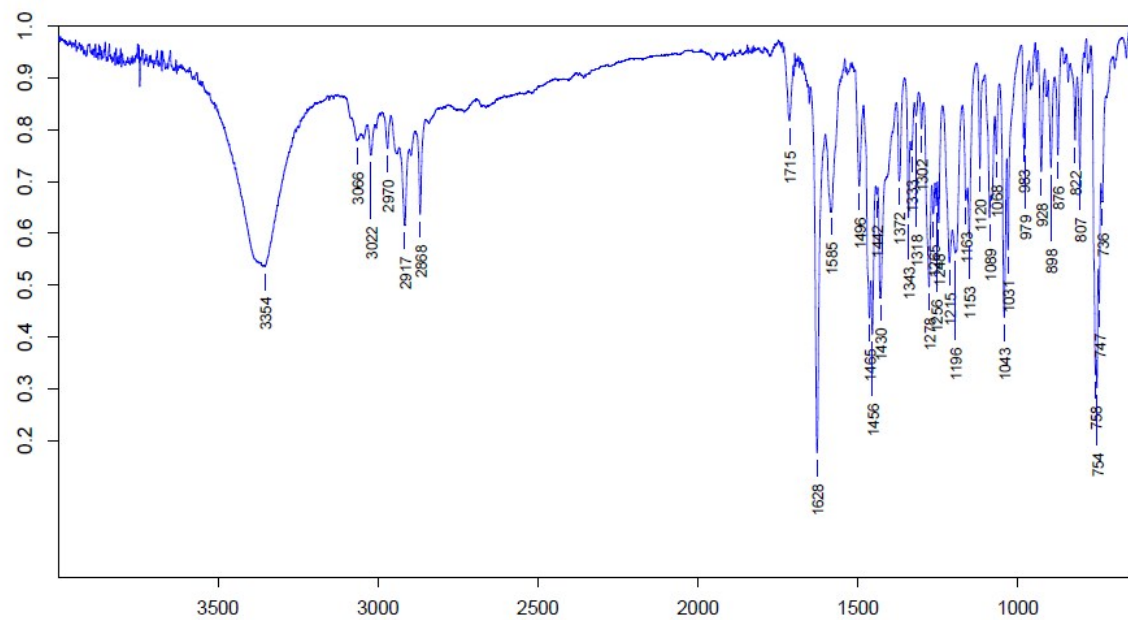


Figure S14. Infrared spectrum of H_2L^1 .

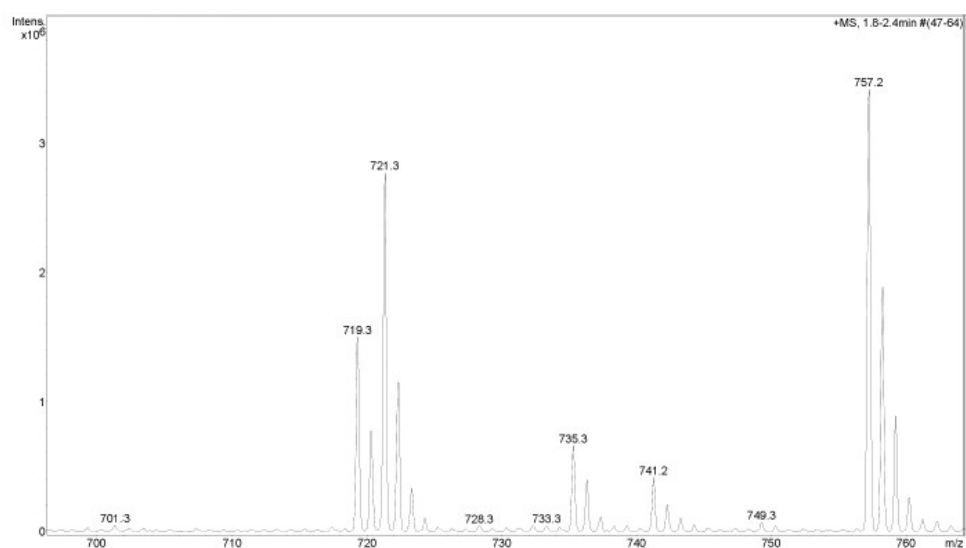
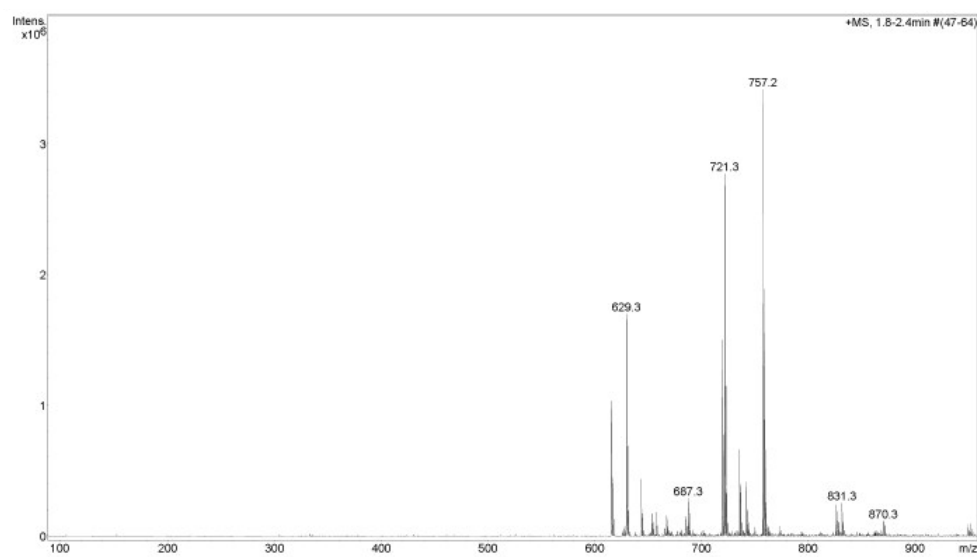


Figure S15. ESI mass spectrum of H_2L^1 .

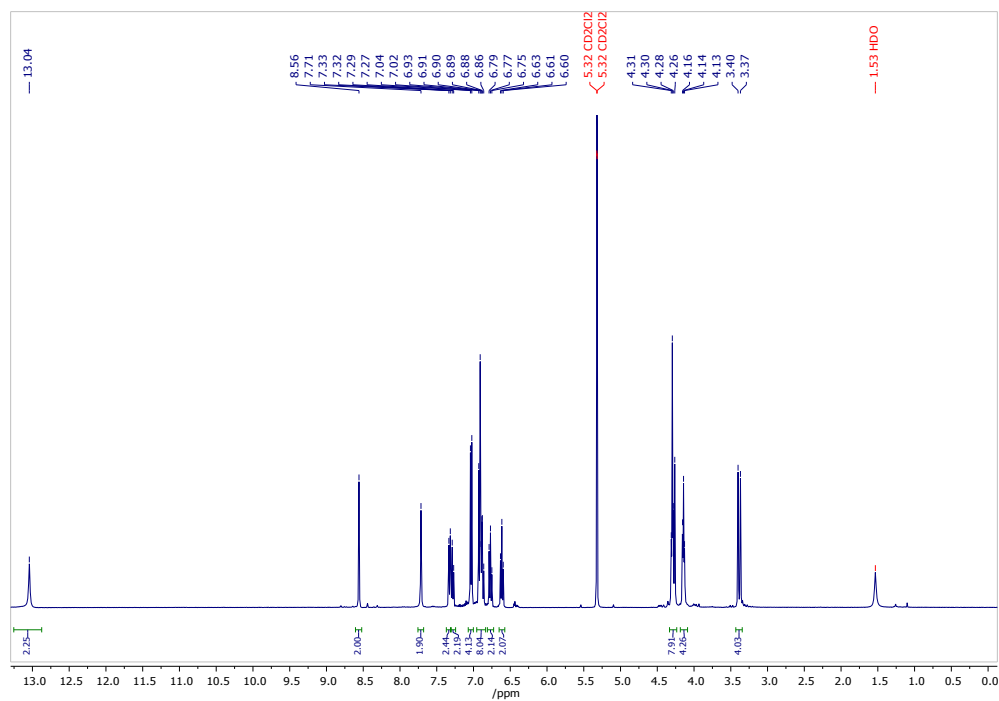


Figure S16: ^1H NMR spectrum of H_2L^1 in CD_2Cl_2 at ambient temperature.

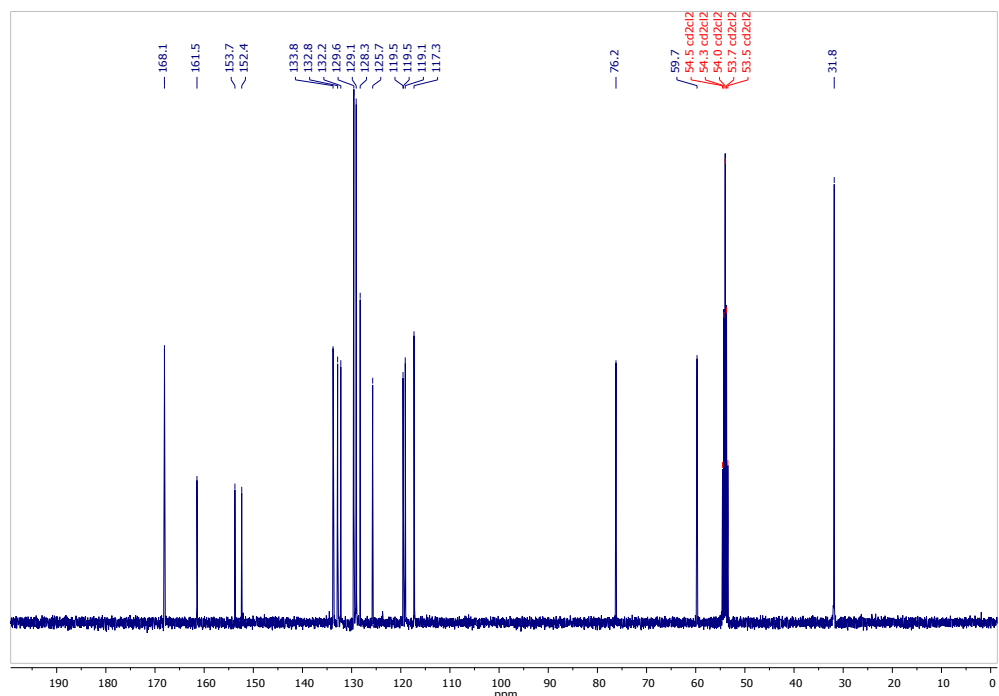


Figure S17: ^{13}C NMR spectrum of H_2L^1 in CD_2Cl_2 at ambient temperature.

cone 25,27-Di[(2'-methylphenol)iminoethoxy]-26,28-di(hydroxy)-calix[4]aren (H_2L^1)

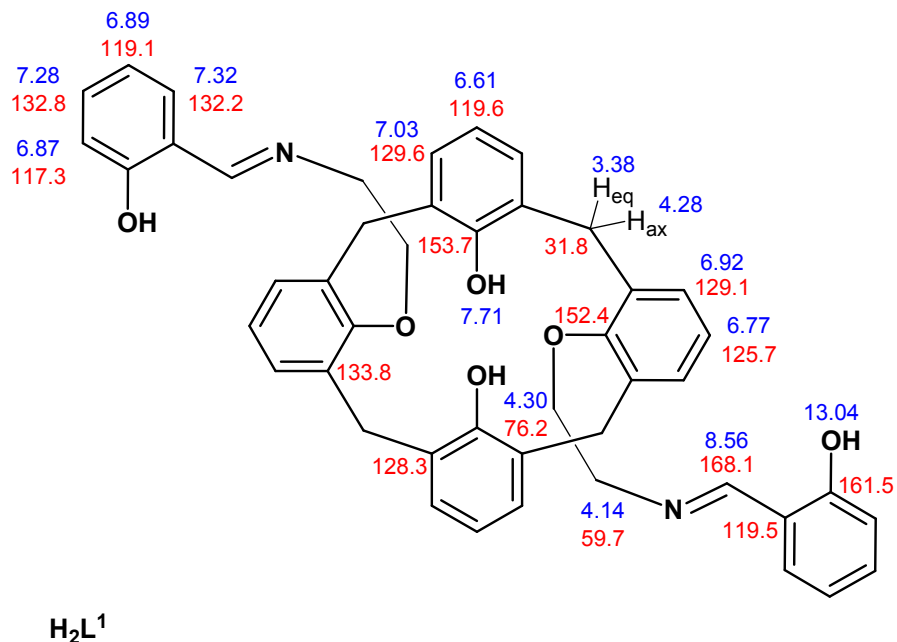


Figure S18. Assignment of NMR signals for H_2L^1 (blue: ^1H , red: ^{13}C)

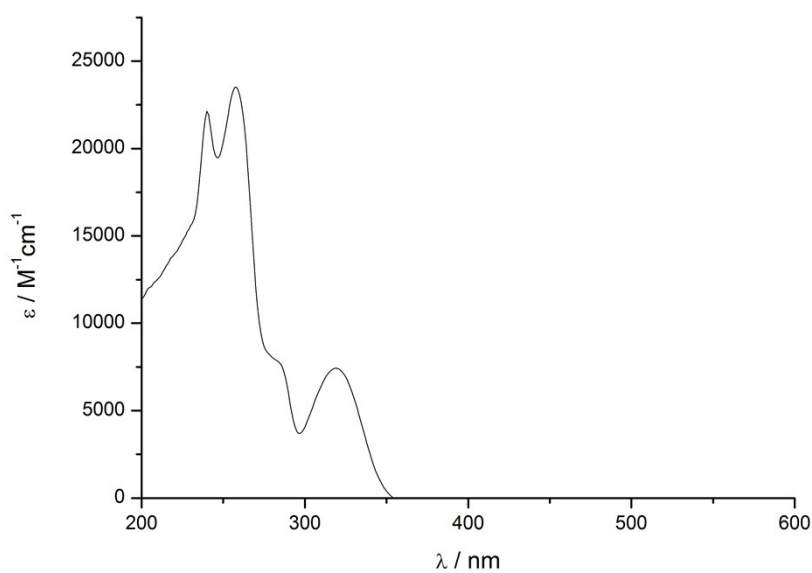


Figure S19. UV/vis spectrum of H_2L^1 in CHCl_3 , $[\text{H}_2\text{L}^1] = 10^{-5} \text{ M}$.

4. Analytical data for compound H₂L².

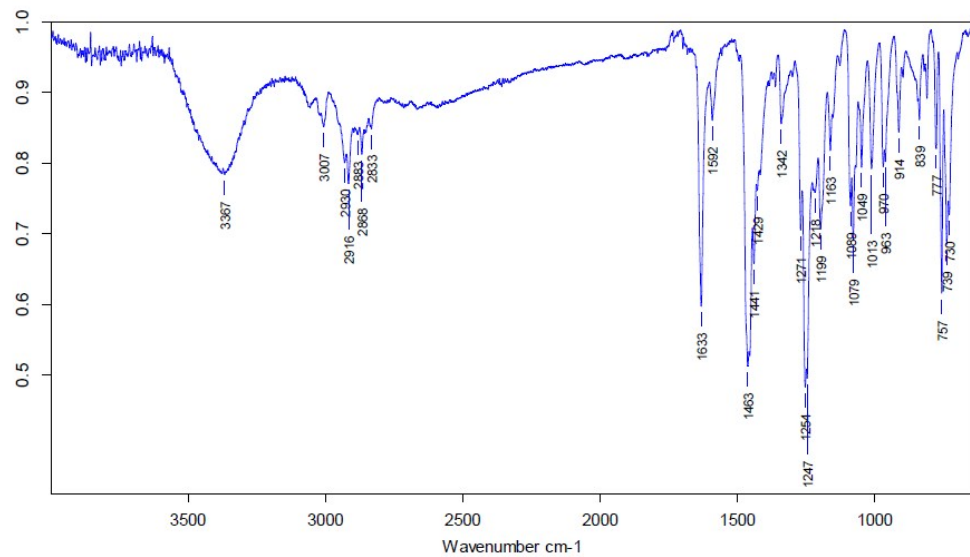
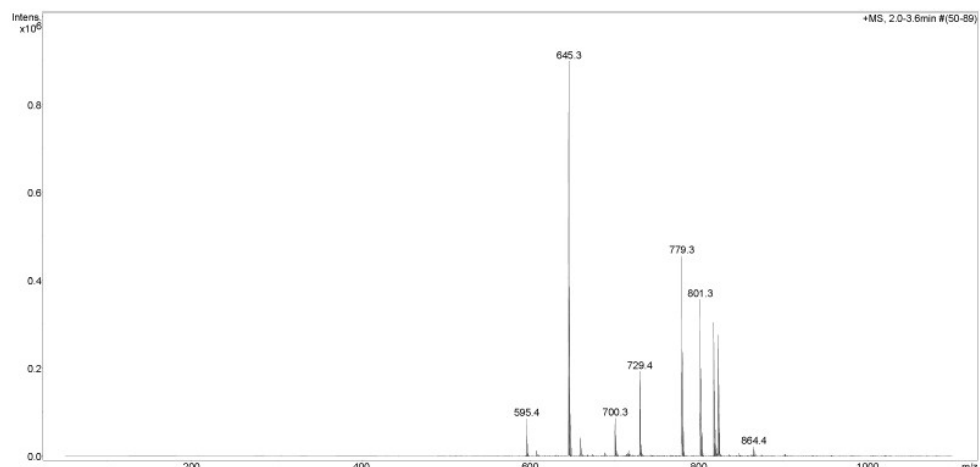


Figure S20. IR spectrum of H₂L².



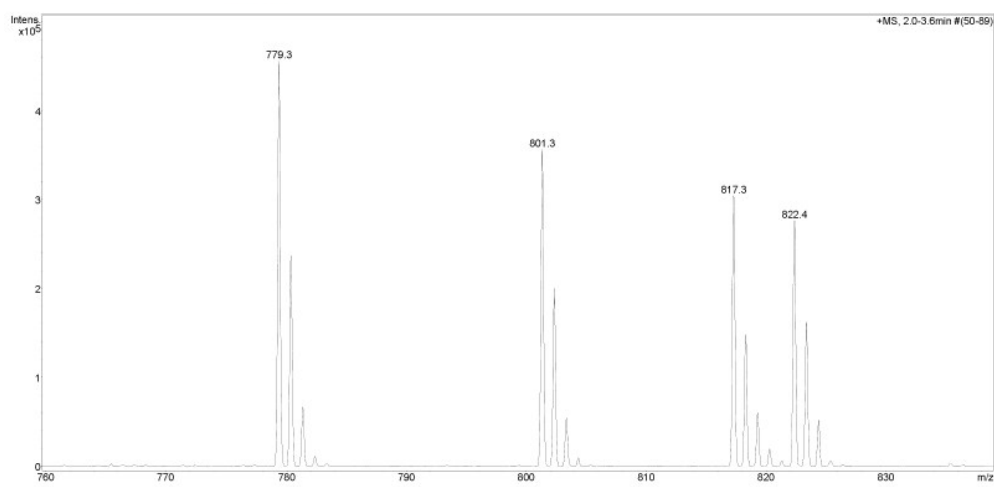


Figure S21. ESI mass spectrum of H_2L^2 in CHCl_3

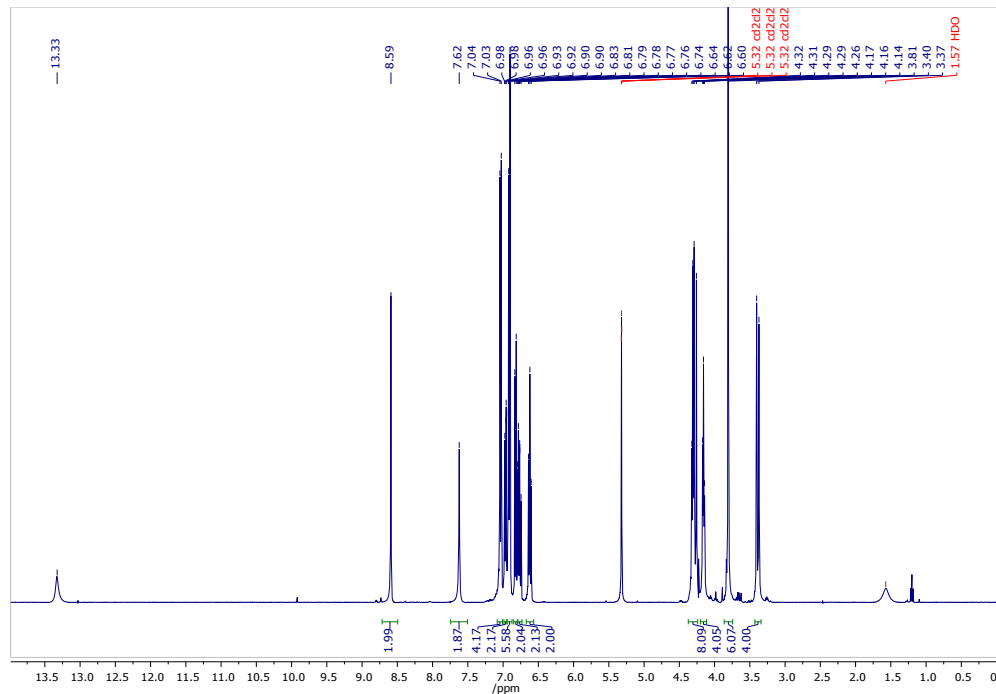


Figure S22: ${}^1\text{H}$ NMR spectrum of H_2L^2 in CD_2Cl_2 at ambient temperature.

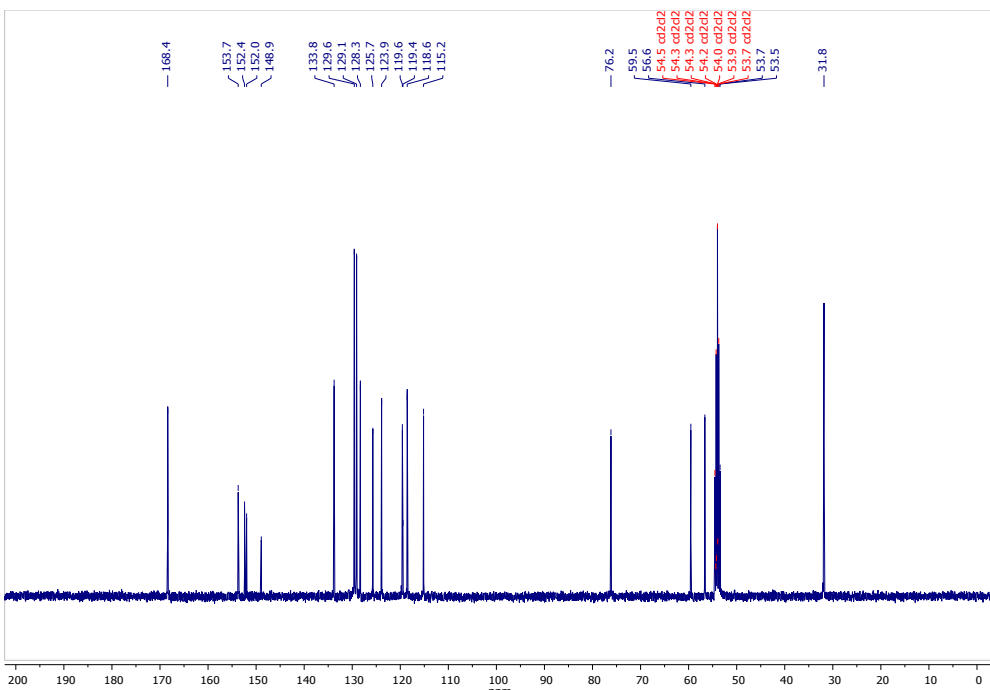


Figure S23: ¹³C NMR spectrum of $\mathbf{H}_2\mathbf{L}^2$ in CD_2Cl_2 at ambient temperature.

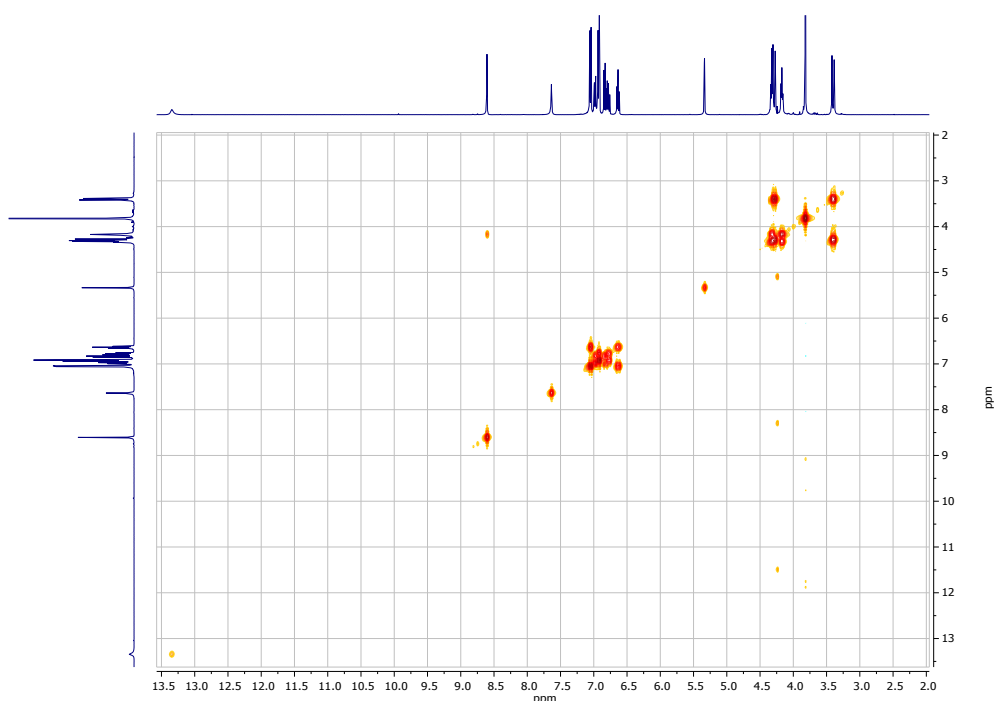


Figure S24: ¹H, ¹H COSY spectrum of $\mathbf{H}_2\mathbf{L}^2$ in CD_2Cl_2 at ambient temperature.

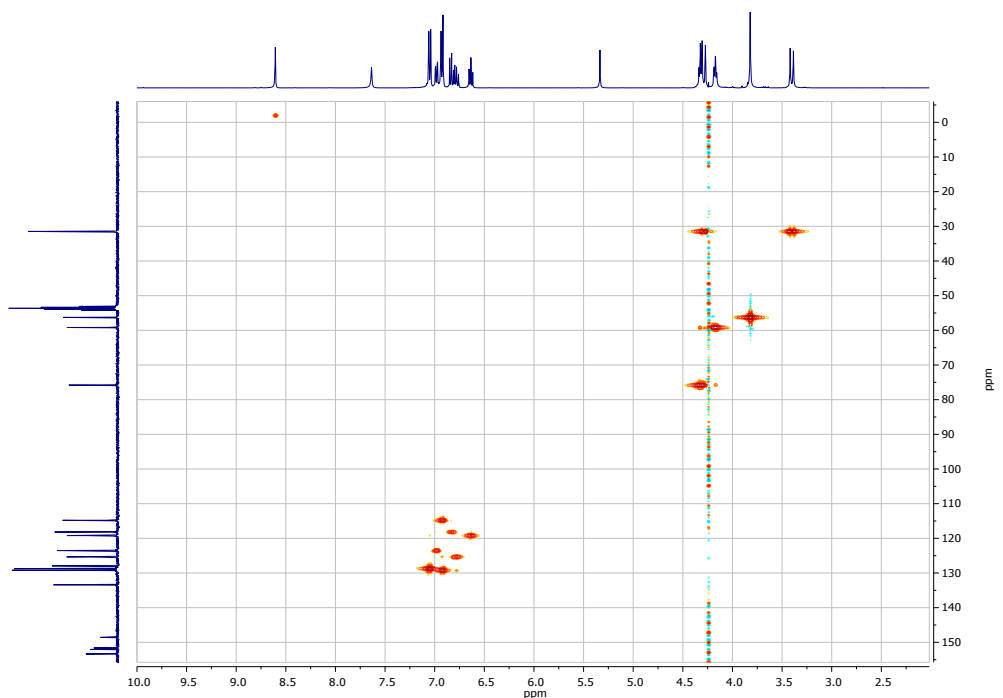


Figure S25: $^1\text{H}, ^{13}\text{C}$ HSQC spectrum of H_2L^2 in CD_2Cl_2 at ambient temperature.

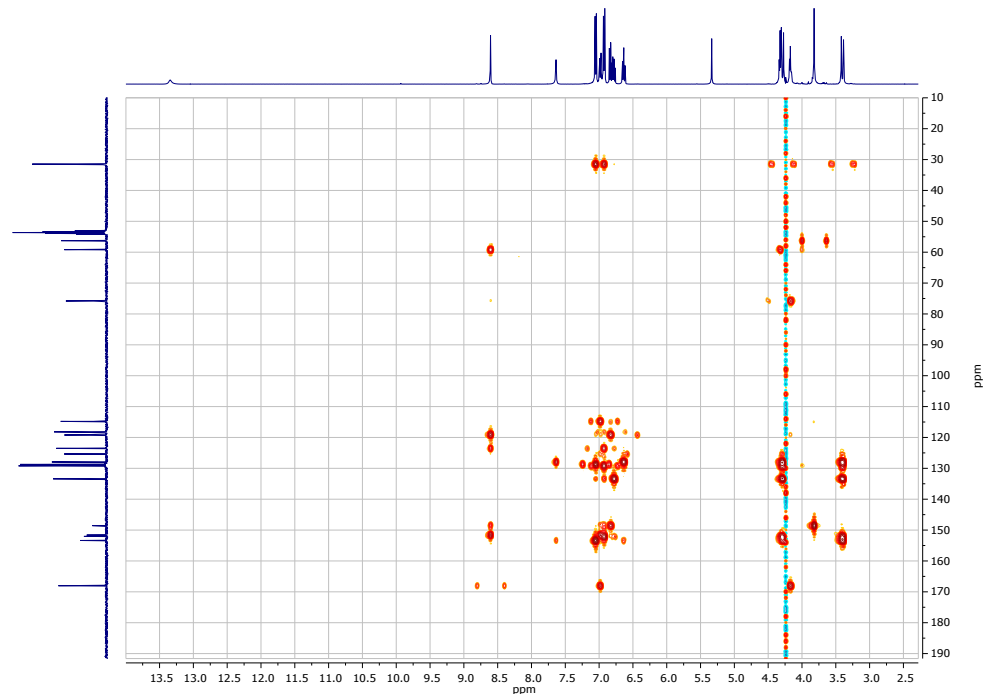


Figure S26: $^1\text{H}, ^{13}\text{C}$ HMBC spectrum of H_2L^2 in CD_2Cl_2 at ambient temperature.

cone 25,27-Di[(2'-methoxy-6'-methylphenol)iminoethoxy]-26,28-di(hydroxy)-calix[4]aren (H_2L^2)

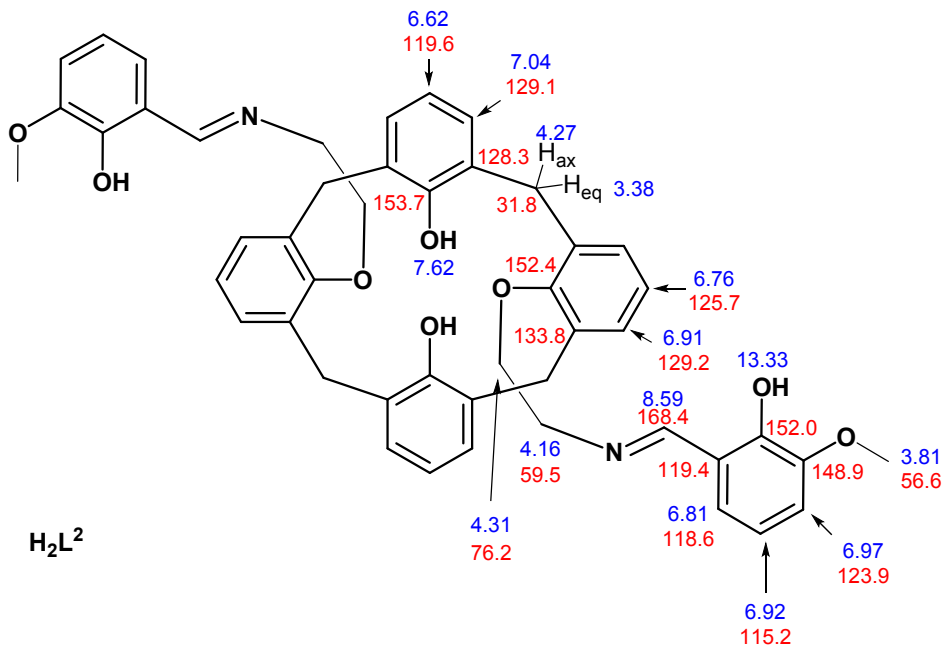


Figure S27. Assignment of NMR signals for $\mathbf{H}_2\mathbf{L}^1$ (blue: ^1H , red: ^{13}C)

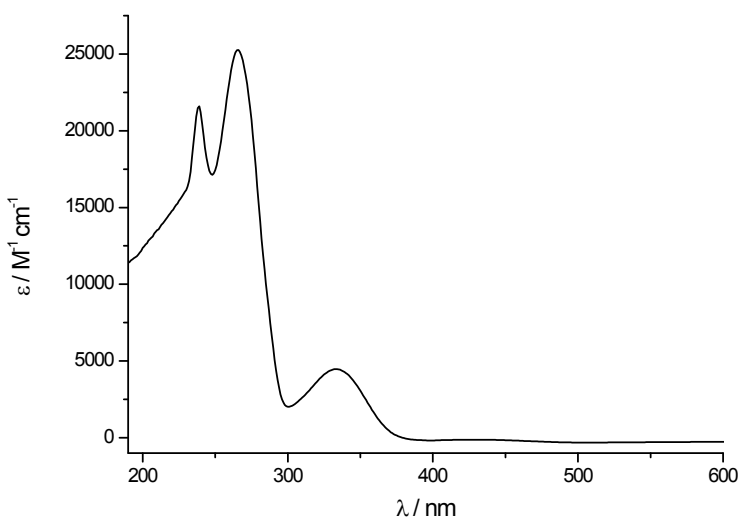


Figure S28. UV/vis spectrum for $\mathbf{H}_2\mathbf{L}^2$ (CHCl_3 , $[\mathbf{H}_2\mathbf{L}^2] = 10^{-5}$ M).

5. Analytical data for compound $\mathbf{H}_2\mathbf{L}^3$.

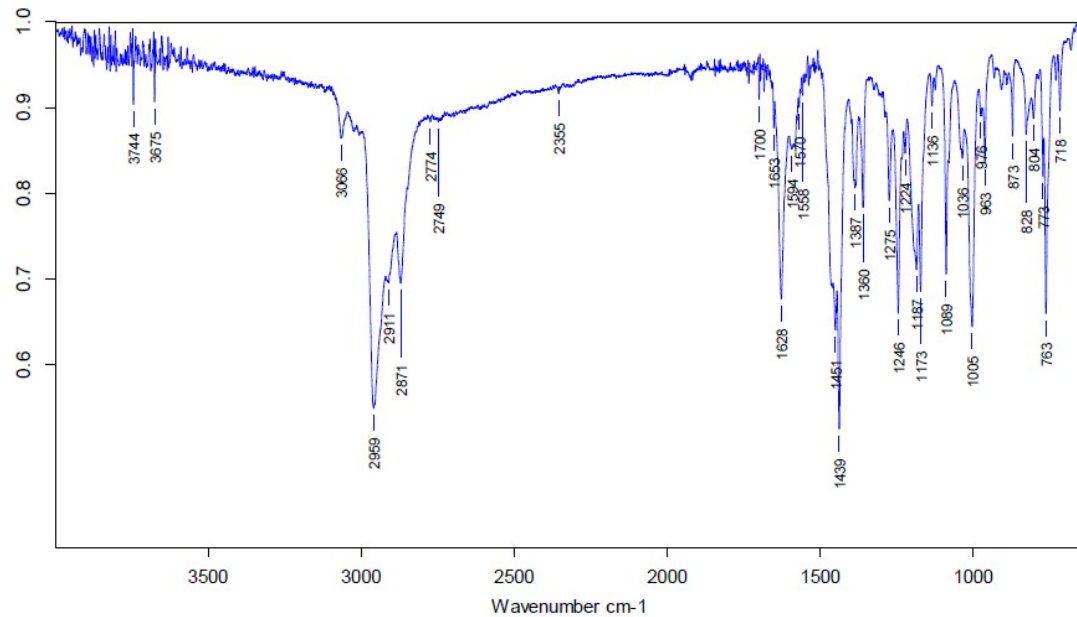


Figure S29. Infrared Spectrum of $\mathbf{H}_2\mathbf{L}^3$.

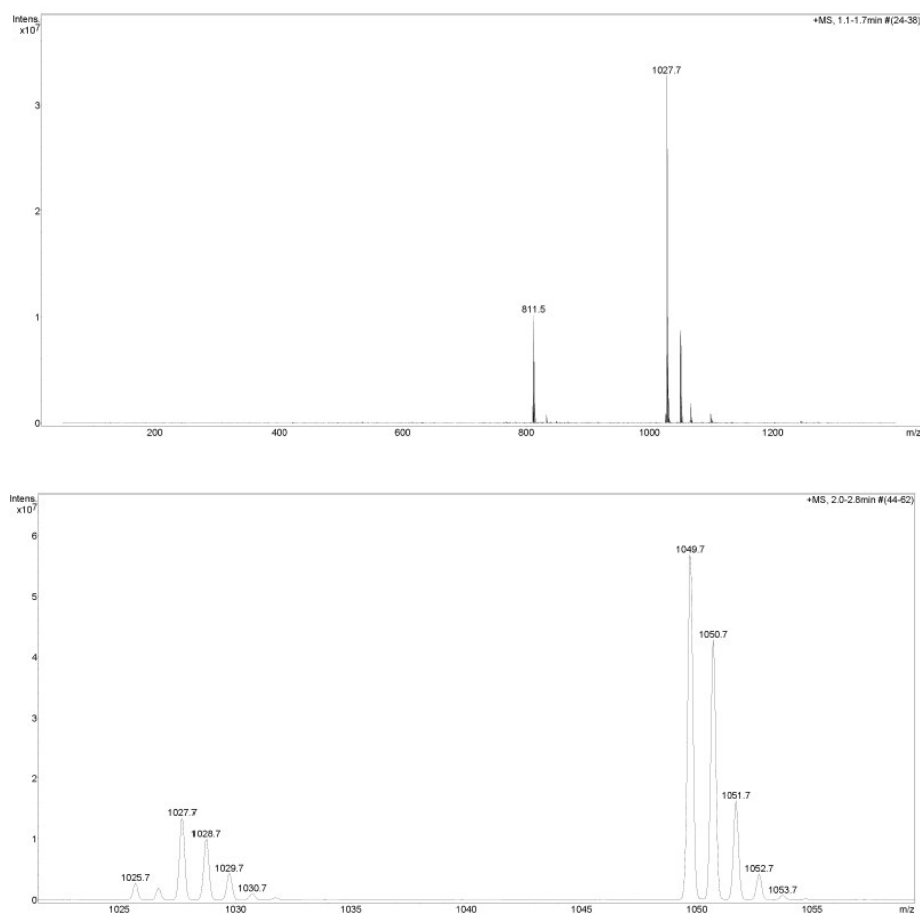


Figure S30: ESI-MS spectrum of H_2L^3 .

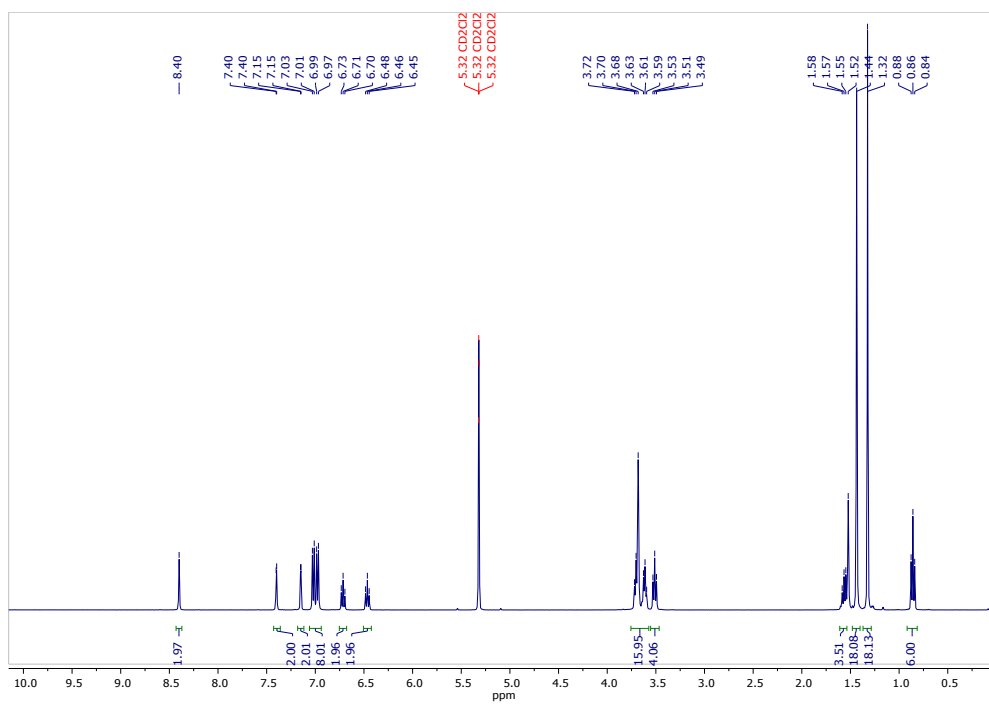


Figure S31: ^1H NMR spectrum of H_2L^3 in CD_2Cl_2 at ambient temperature.

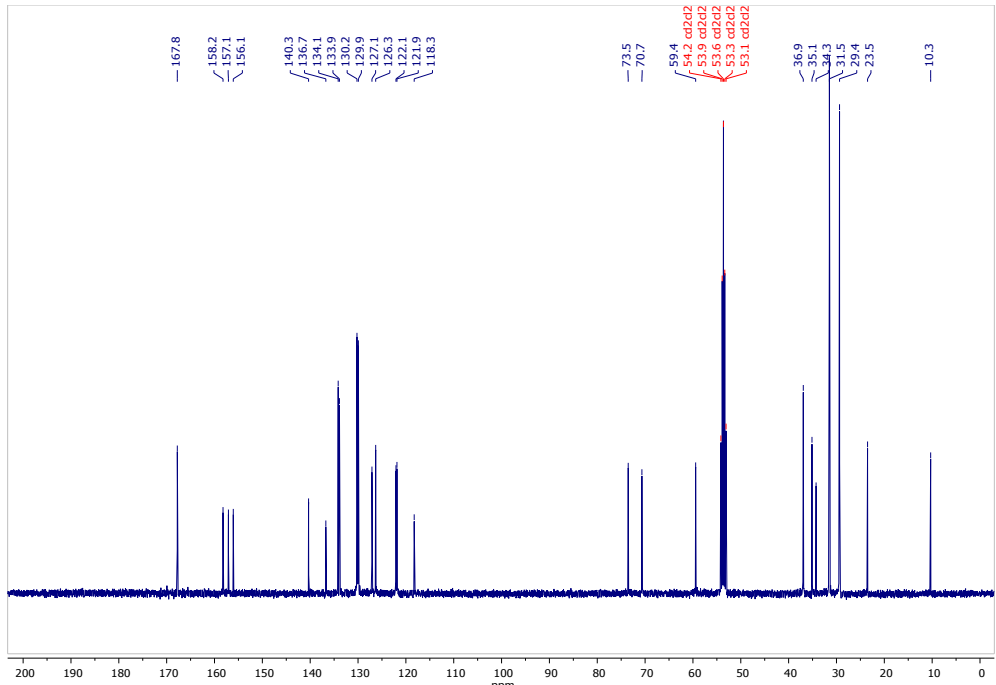


Figure S32: ¹³C NMR spectrum of $\mathbf{H}_2\mathbf{L}^3$ in CD_2Cl_2 at ambient temperature.

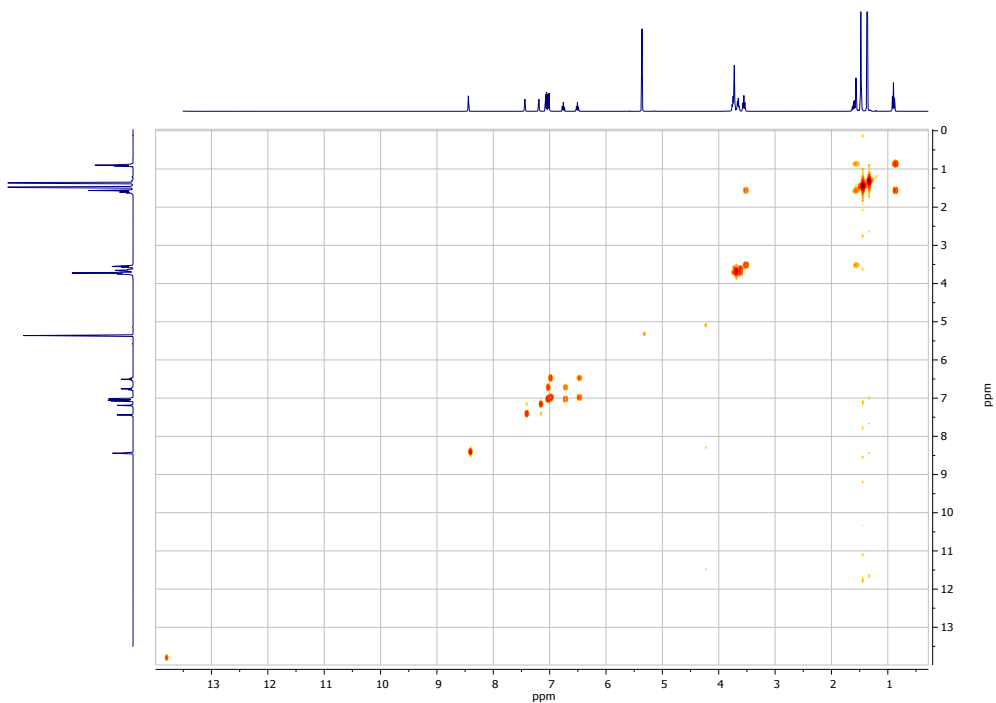


Figure S33: ¹H, ¹H COSY spectrum of $\mathbf{H}_2\mathbf{L}^3$ in CD_2Cl_2 at ambient temperature.

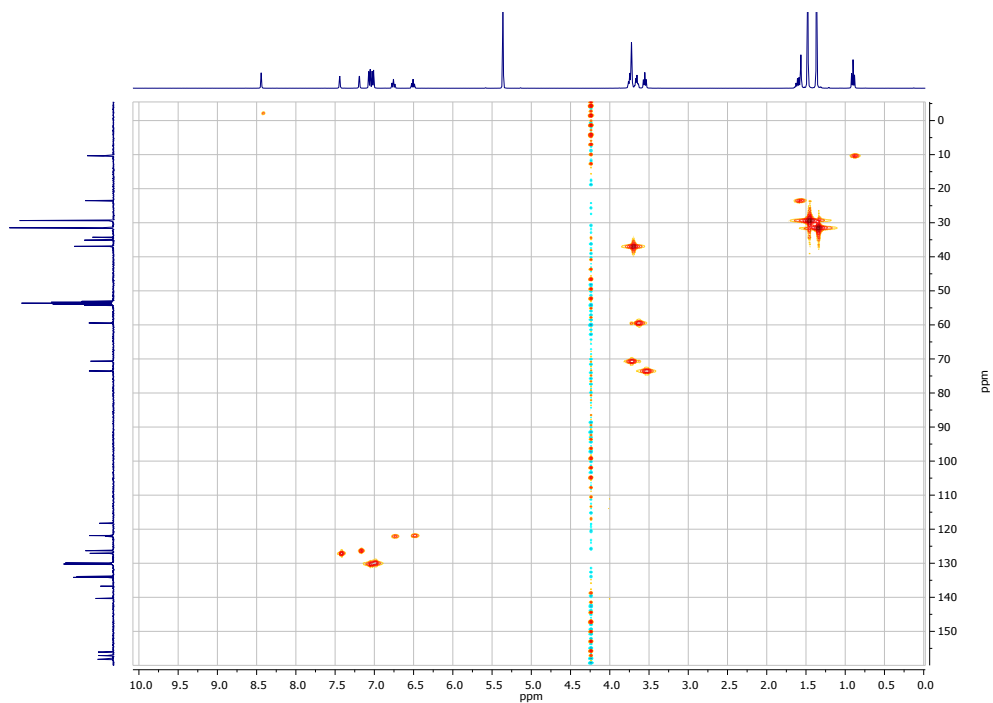


Figure S34: $^1\text{H}, ^{13}\text{C}$ HSQC spectrum of H_2L^3 in CD_2Cl_2 at ambient temperature.

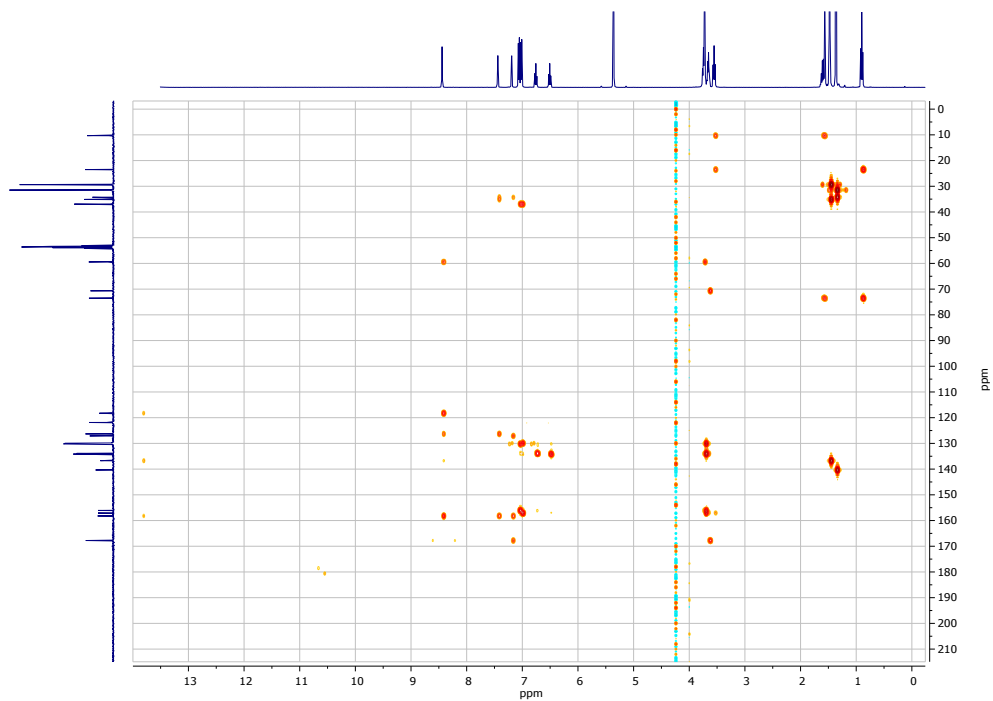


Figure S35: $^1\text{H}, ^{13}\text{C}$ HMBC spectrum of H_2L^3 in CD_2Cl_2 at ambient temperature.

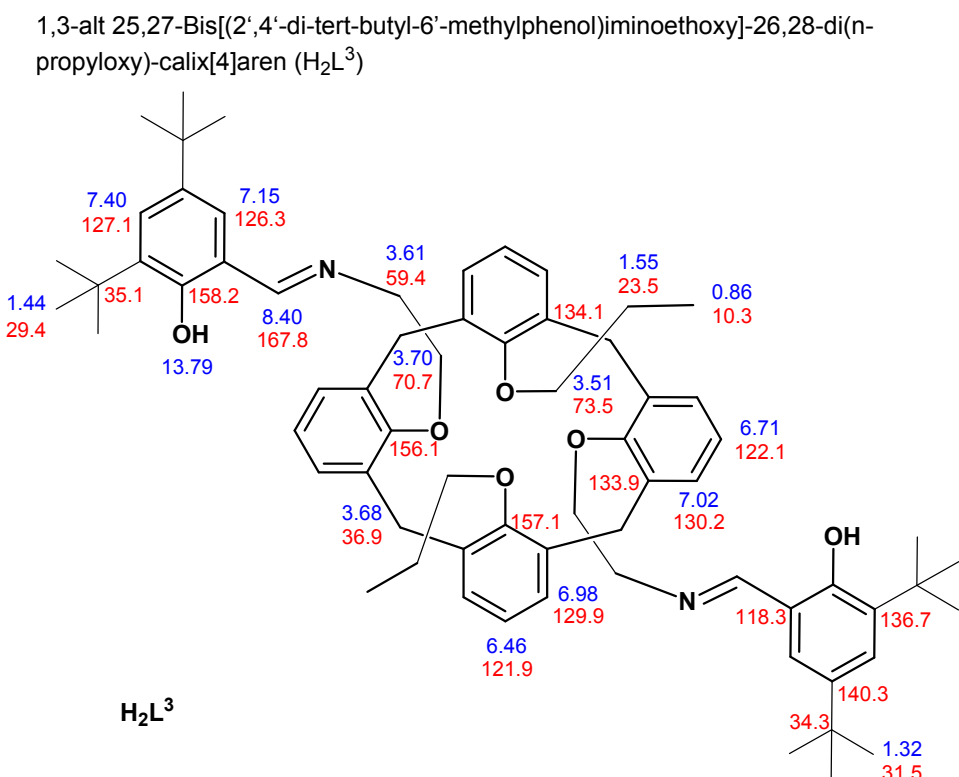


Figure S36. Assignment of NMR signals for H_2L^1 (blue: ^1H , red: ^{13}C)

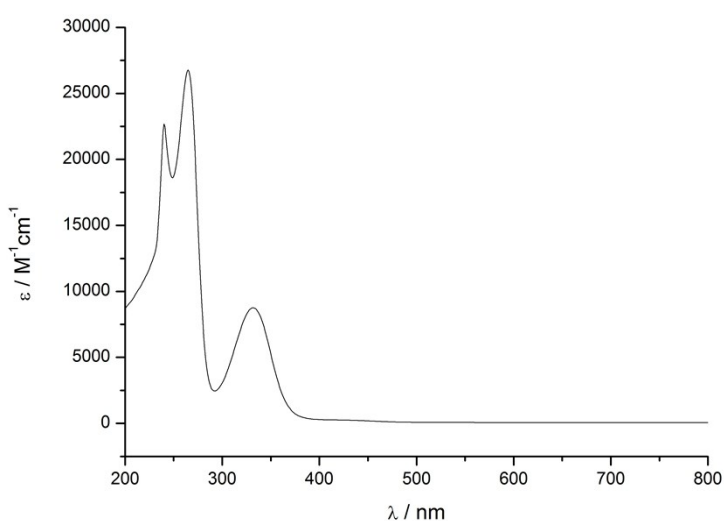


Figure S37. UV/vis spectrum for H_2L^3 (CHCl_3 , $[\text{H}_2\text{L}^2] = 10^{-5}$ M).

6) Analytical Data for Compound H₂L⁴.

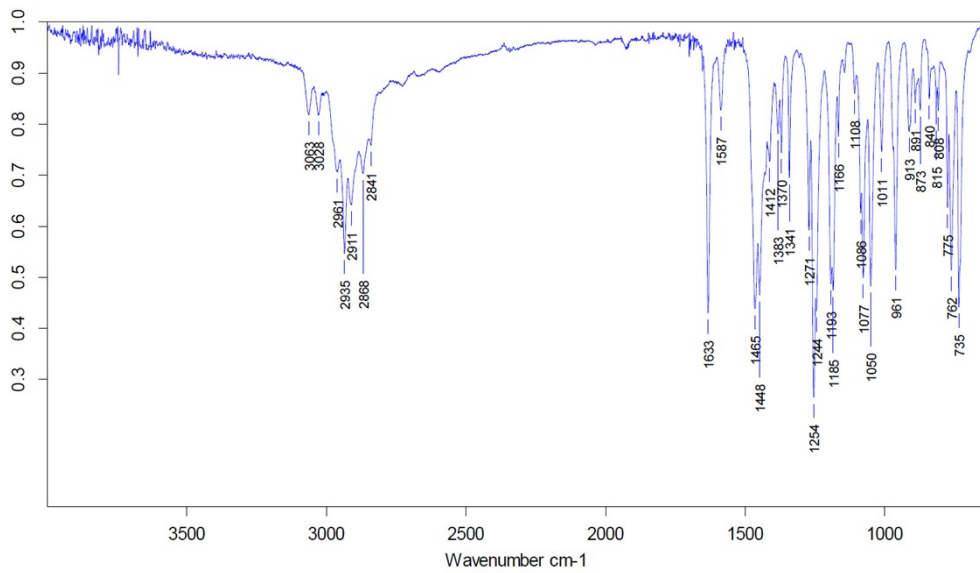


Figure S38. Infrared spectrum for H₂L⁴.

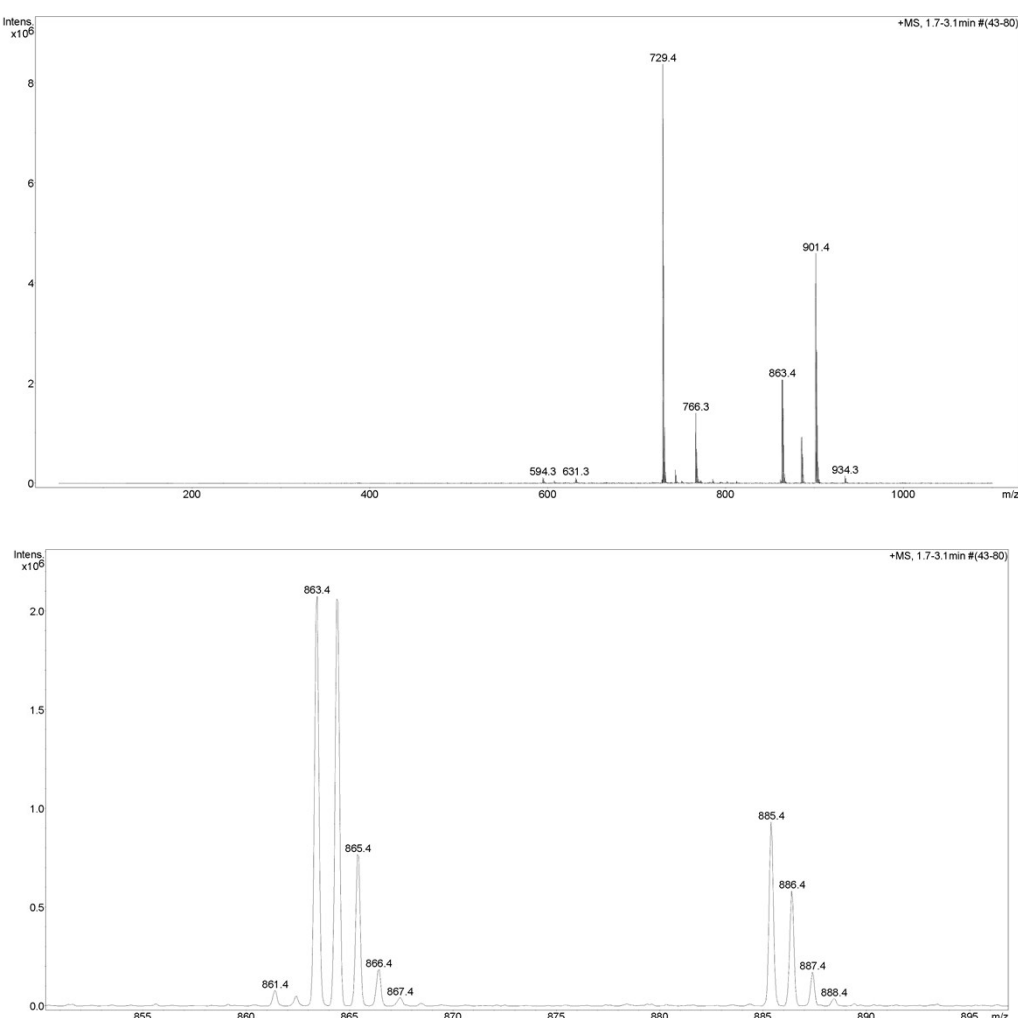


Figure S39. ESI-MS spectrum for H₂L⁴.

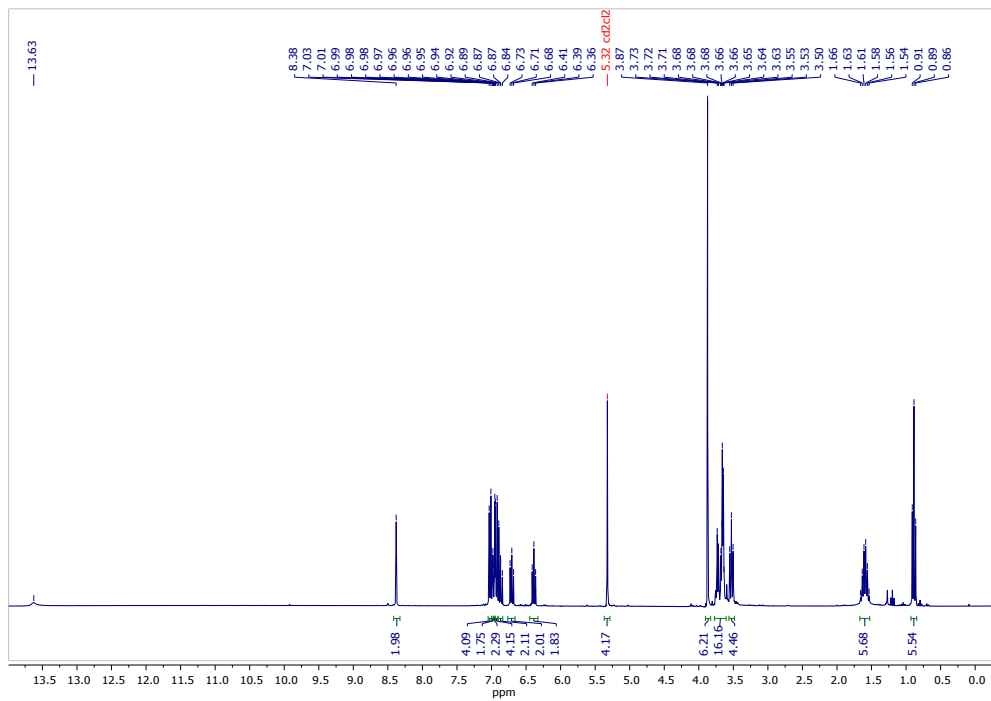


Figure S40: ^1H NMR spectrum of H_2L^4 in CD_2Cl_2 at ambient temperature.

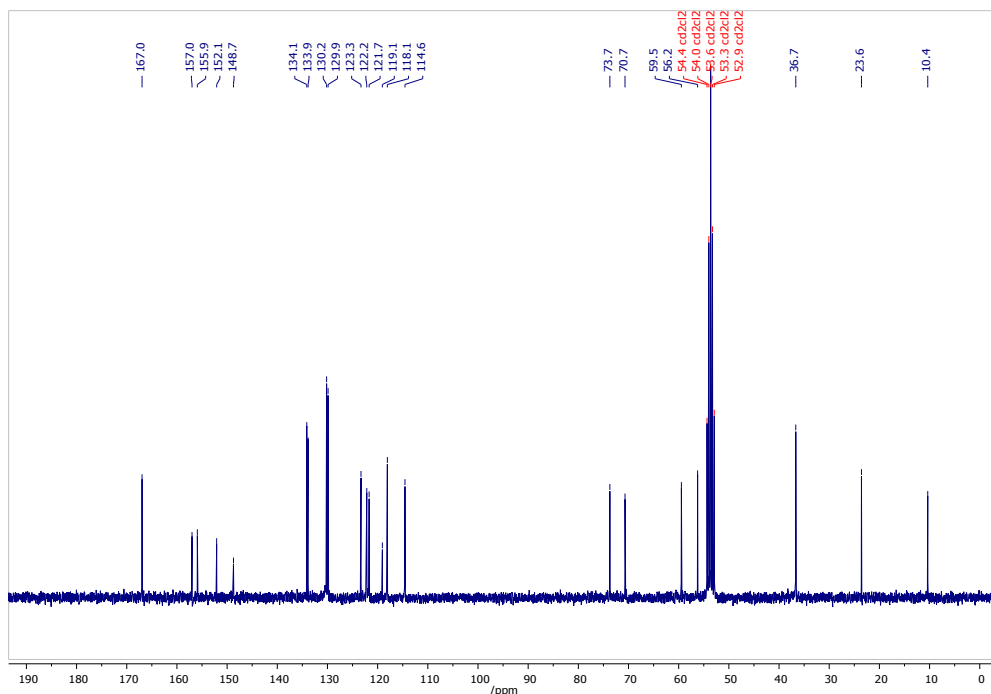


Figure S41: ^{13}C NMR spectrum of H_2L^4 in CD_2Cl_2 at ambient temperature.

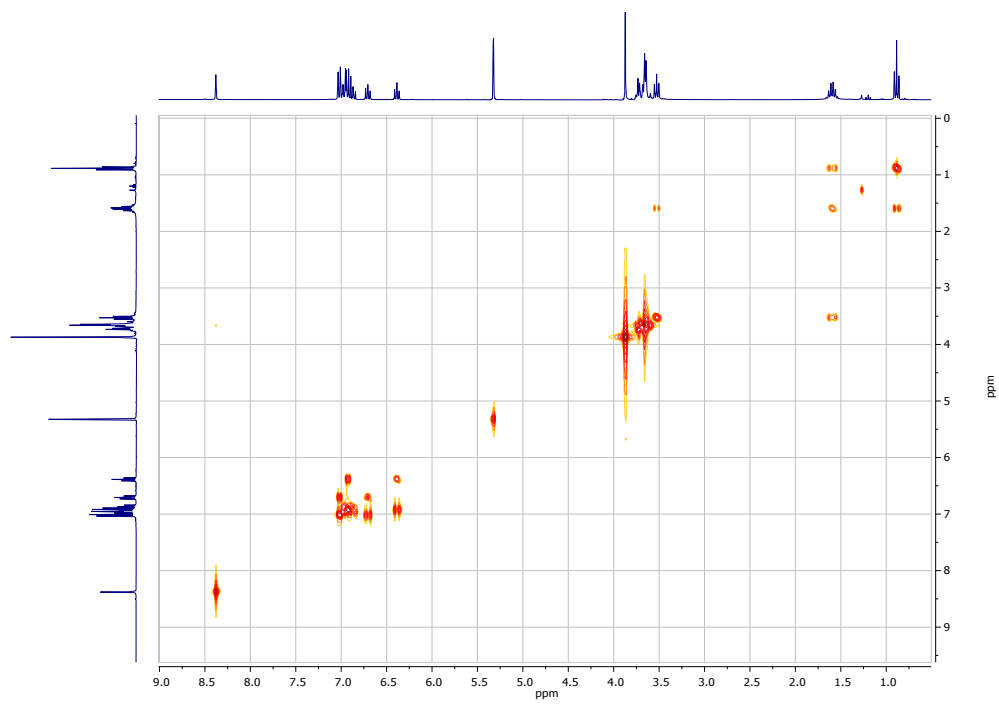


Figure S42: ¹H, ¹H COSY spectrum of $\mathbf{H}_2\mathbf{L}^4$ in CD_2Cl_2 at ambient temperature.

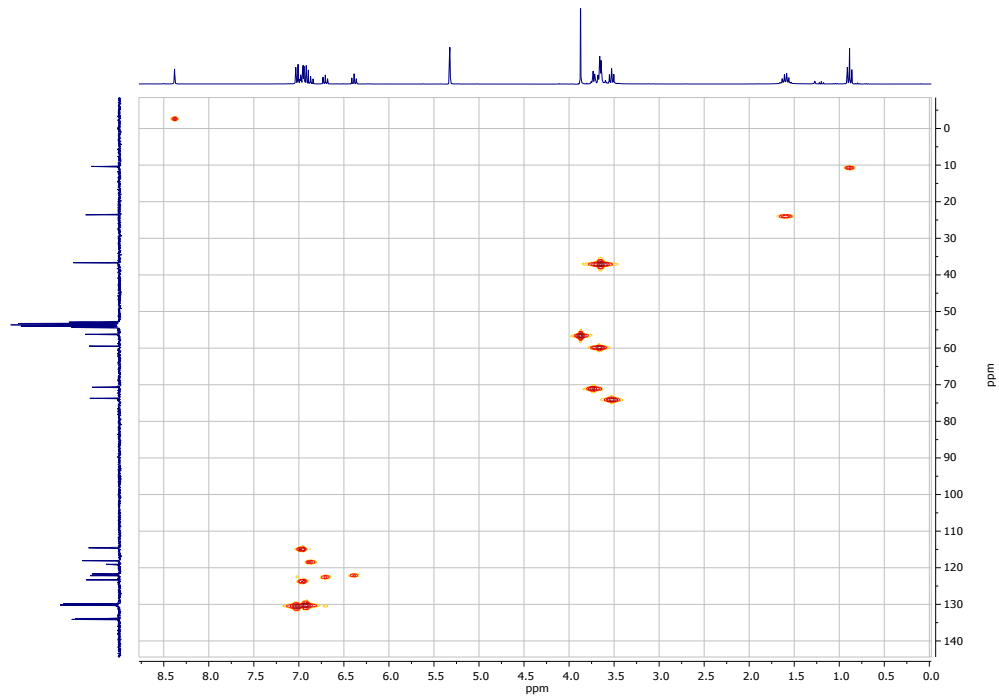


Figure S43: ¹H, ¹³C HSQC spectrum of $\mathbf{H}_2\mathbf{L}^4$ in CD_2Cl_2 at ambient temperature.

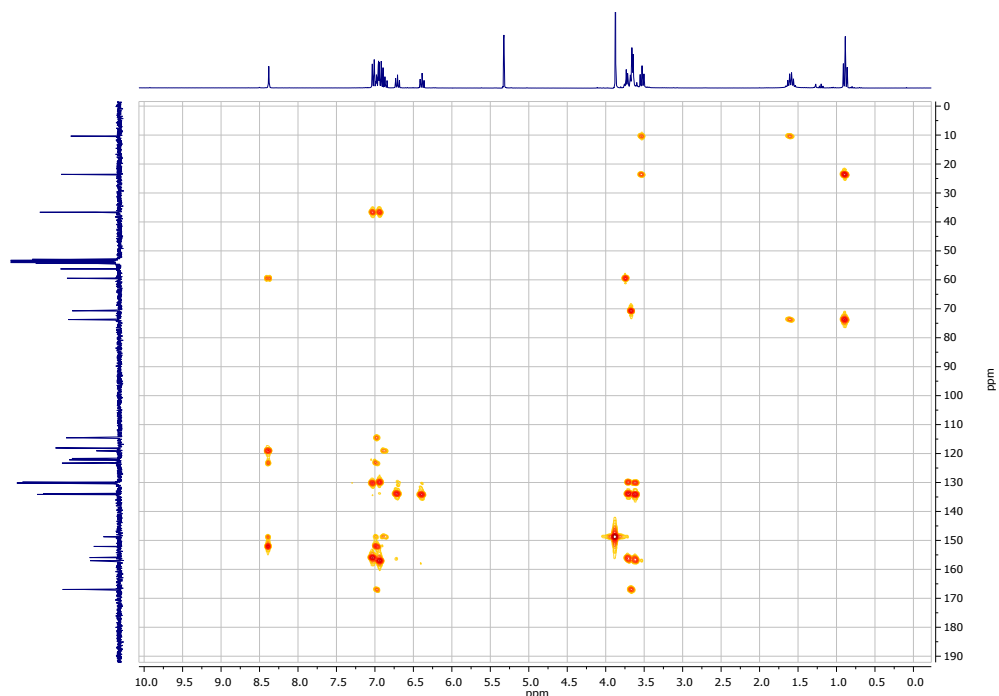


Figure S44: ^1H , ^{13}C HMBC spectrum of H_2L^4 in CD_2Cl_2 at ambient temperature.

1,3-alt 25,27-di[(2'-methoxy-6'-methylphenol)iminoethoxy]-26,28-di(n-propyloxy)-calix[4]aren (H_2L^4)

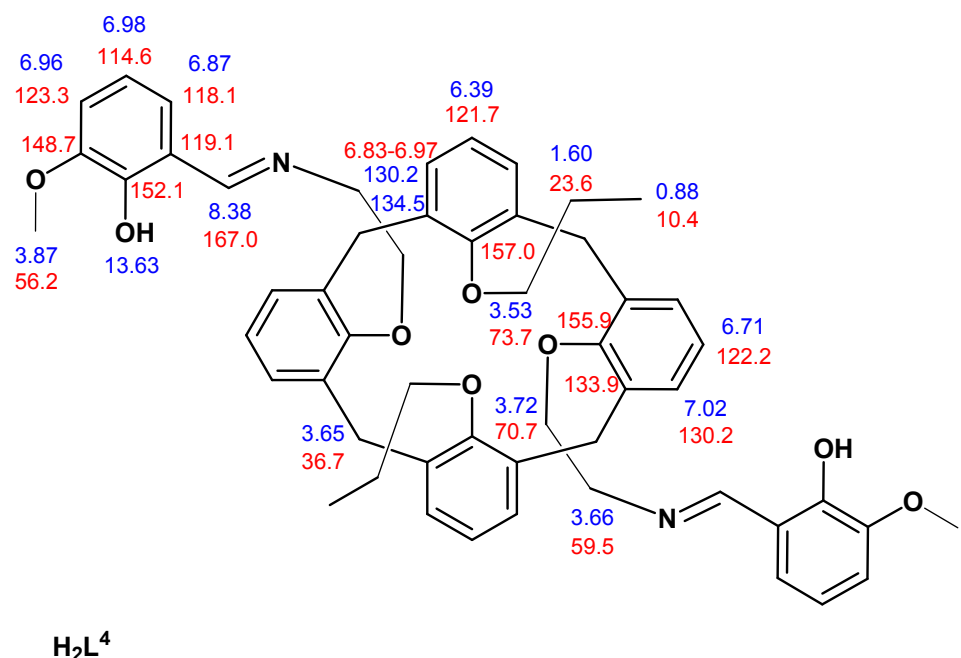


Figure S45. Assignment of NMR signals for H_2L^1 (blue: ^1H , red: ^{13}C)

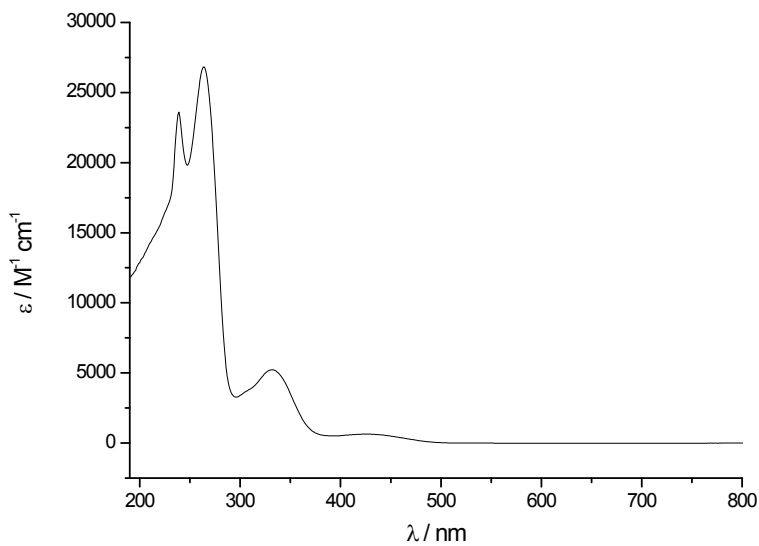


Figure S46. UV/Vis spectrum for $\mathbf{H}_2\mathbf{L}^4$ CHCl_3 , $[\mathbf{H}_2\mathbf{L}^4] = 10^{-5}$ M

7) Fluorescence spectra of $\mathbf{H}_2\mathbf{L}^1$ - $\mathbf{H}_2\mathbf{L}^4$

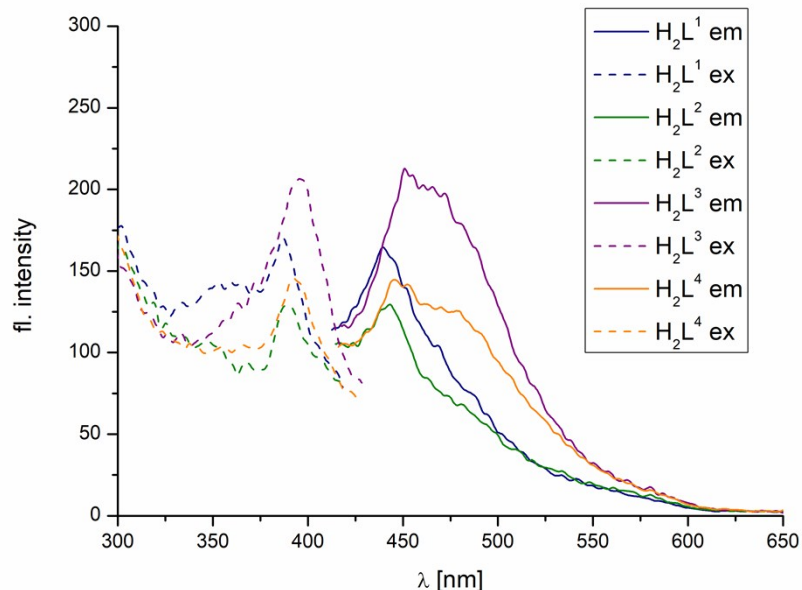


Figure S47: Steady state fluorescence absorption and emission data of $\mathbf{H}_2\mathbf{L}^1$ - $\mathbf{H}_2\mathbf{L}^4$ in dichloromethane/acetonitrile solution (1/1 : v/v). Concentration of solutions 1×10^{-5} M, $T = 298$ K.

8) Analytical data for $[Zn(L^1)]$

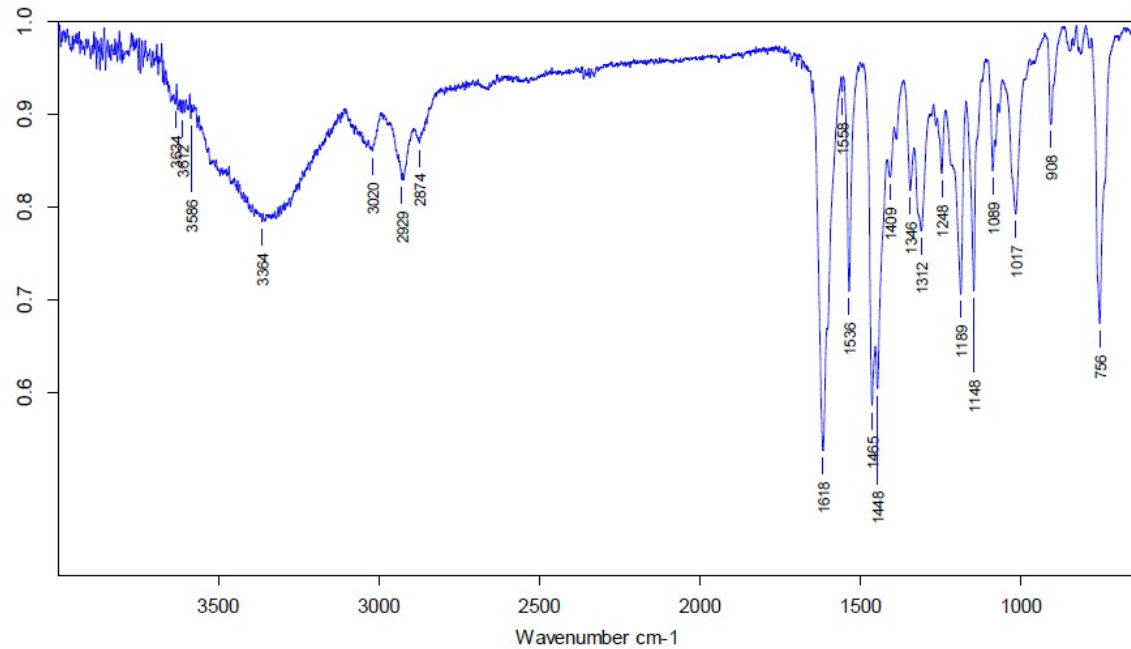


Figure S48. Infrared spectrum for $[ZnL^1]$.

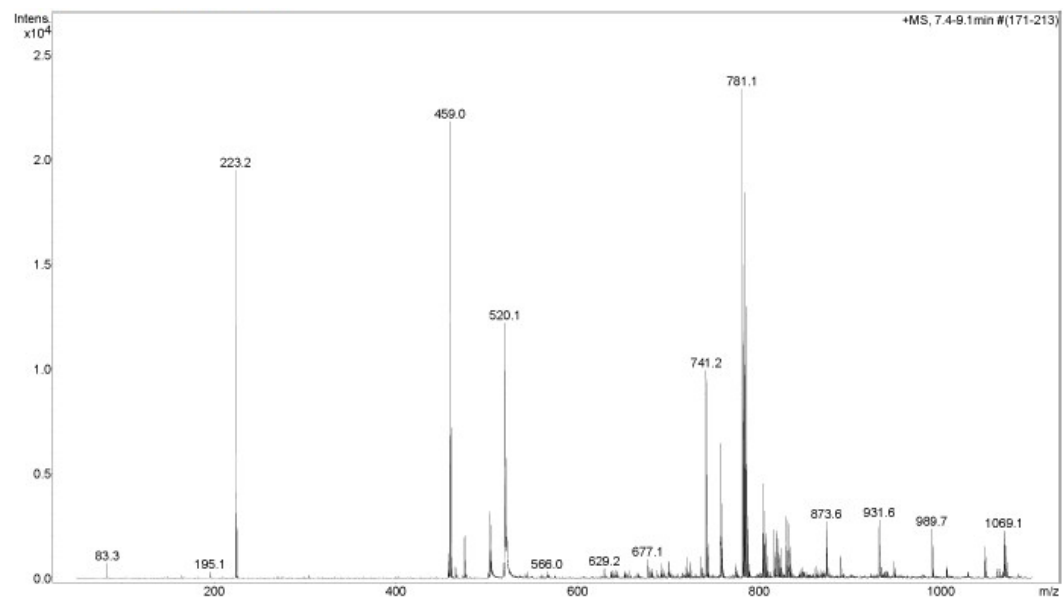


Figure S49. ESI mass spectrum of $[ZnL^1]$.

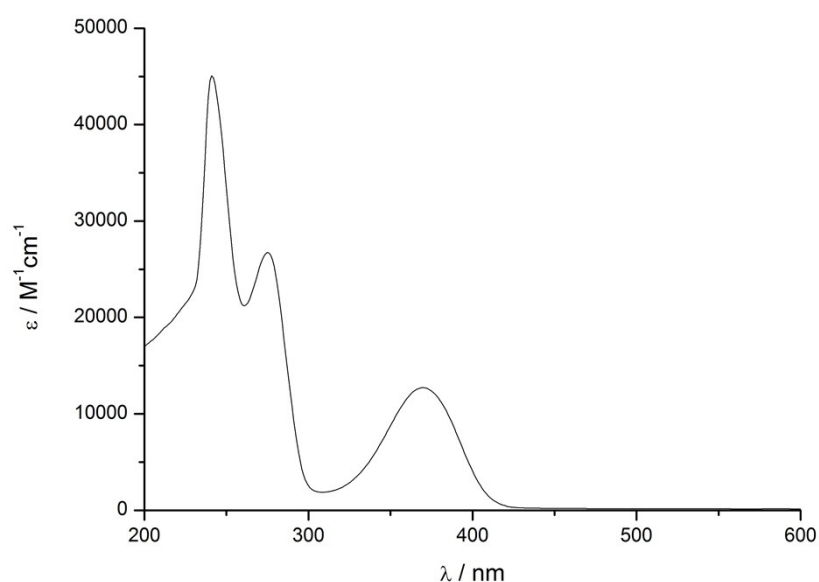
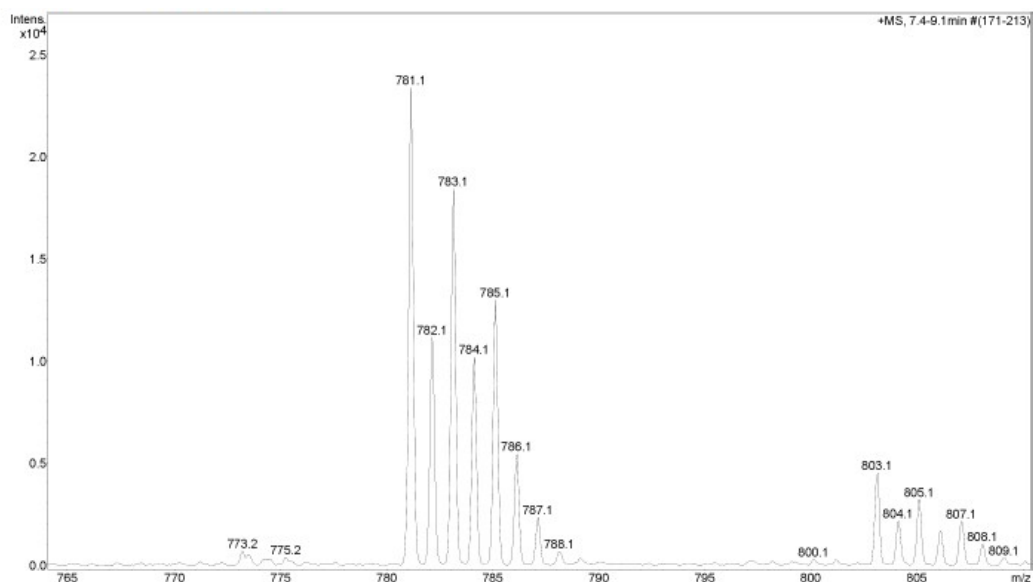


Figure S50. UV/Vis spectrum of $[ZnL^1]$ ($CHCl_3$, $[ZnL^1] = 10^{-5} M$).

9) Analytical data for $[Zn(L^2)]$

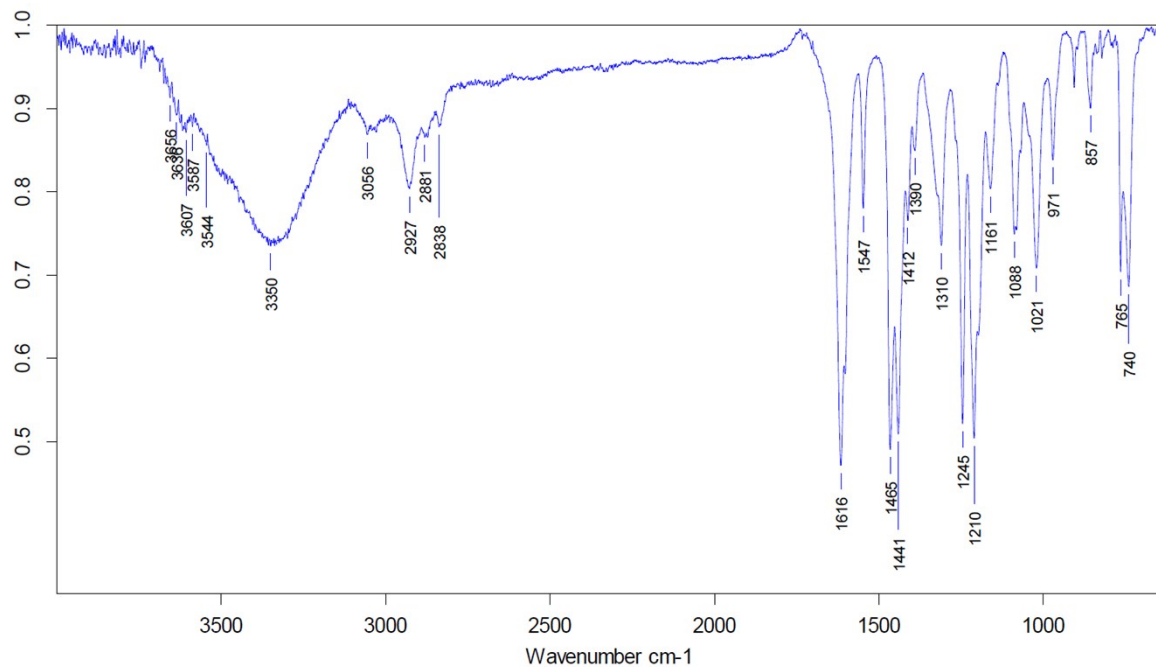


Figure S51. Infrared spectrum for ZnL^2 (KBr pellet).

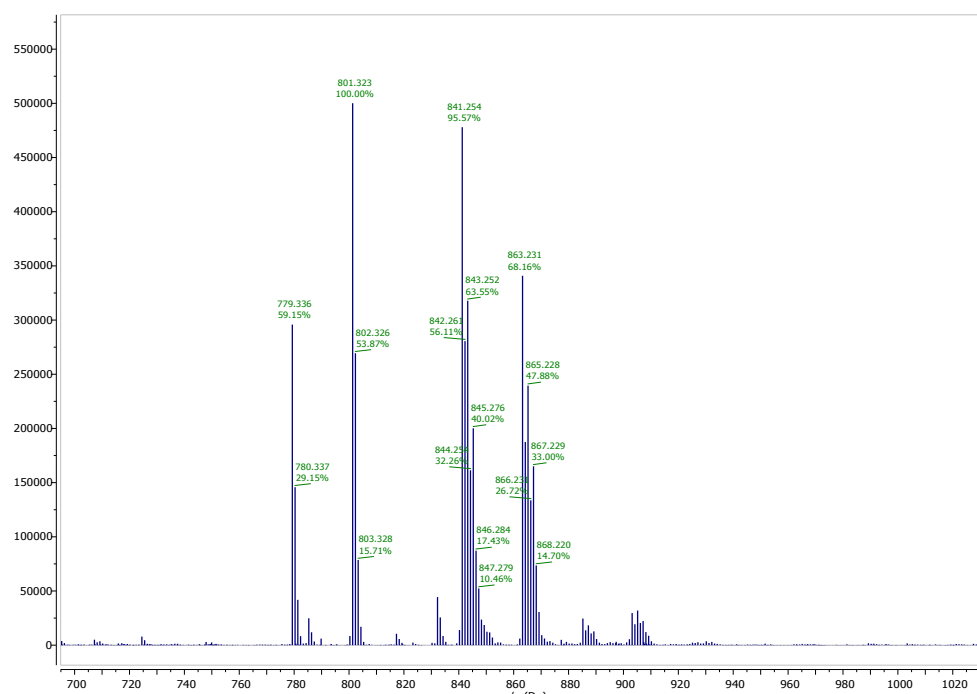


Figure S52a. ESI mass spectrum for ZnL^2 .

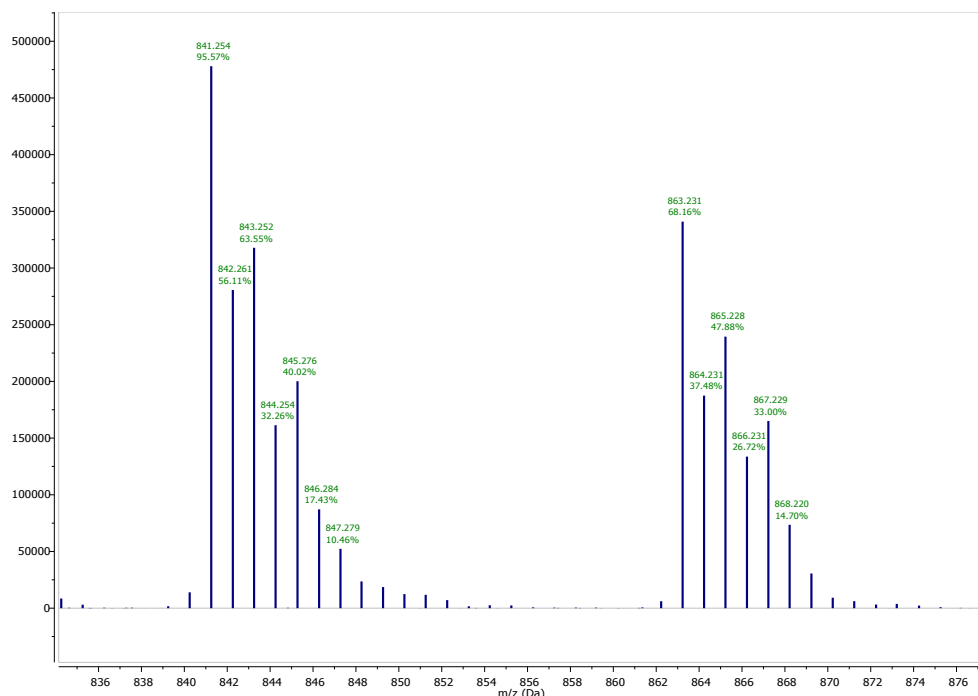


Figure S52b. ESI mass spectrum for ZnL^2 .

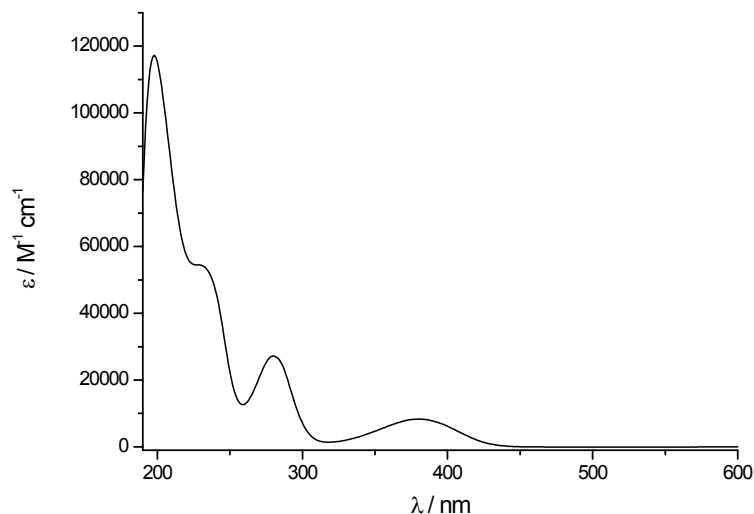


Figure S53. UV/Vis spectrum for ZnL^2 (MeCN, $[\text{ZnL}^2] = 2,5 \cdot 10^{-5} \text{ M}$)

10) Analytical data for $[\text{ZnL}^3]$

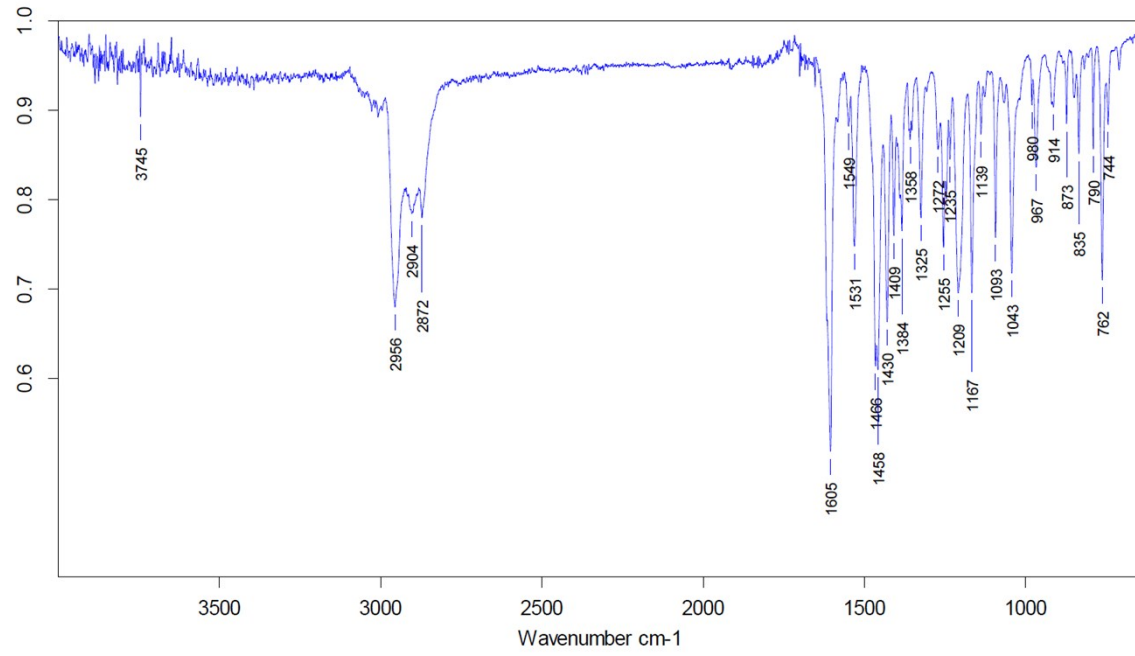


Figure S54. Infrared spectrum for ZnL^2 (KBr pellet).

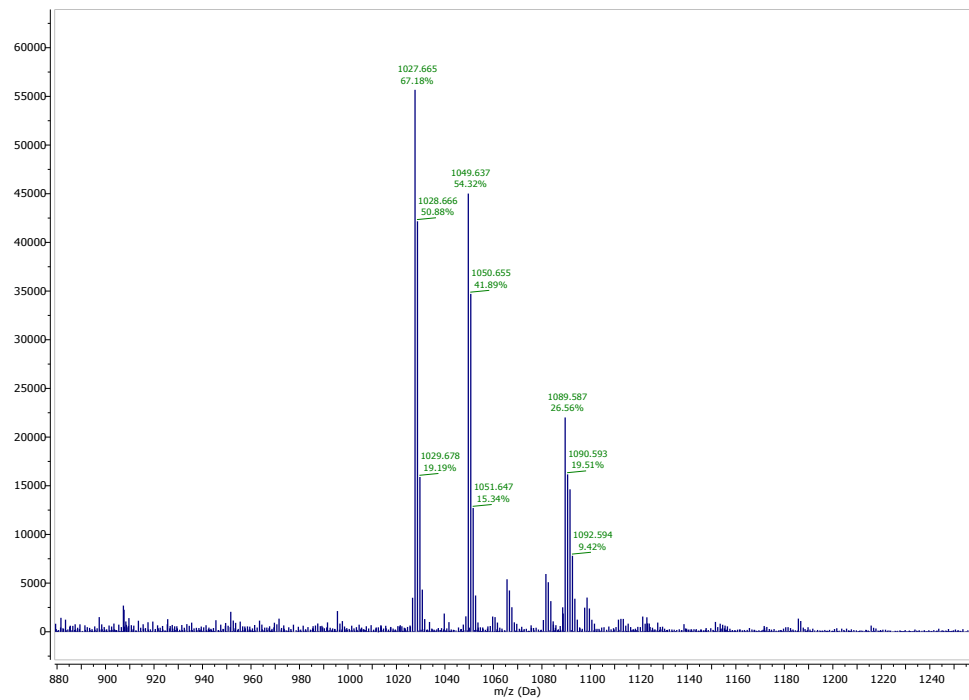


Figure S54. ESI mass spectrum for ZnL^3 .

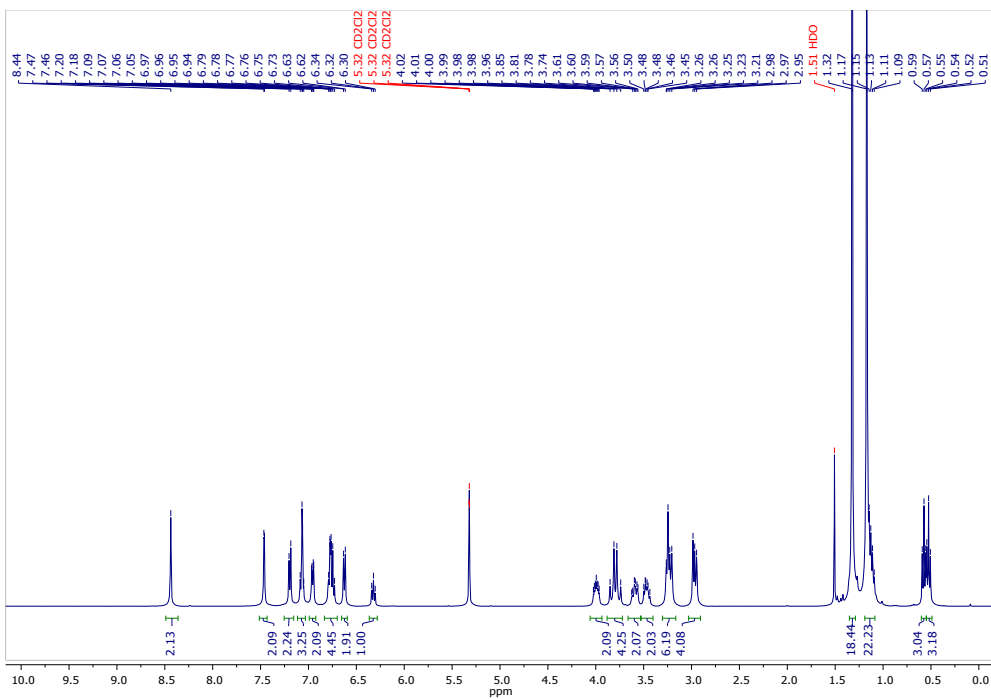


Figure S55: ^1H NMR spectrum of $[\text{ZnL}^3]$ in CD_2Cl_2 at ambient temperature.

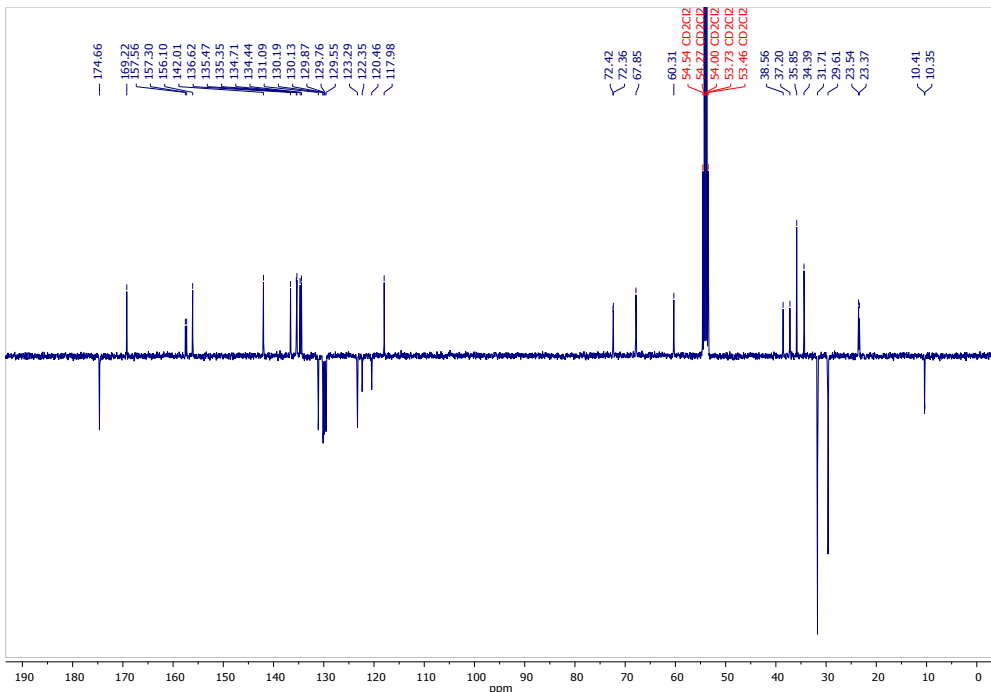


Figure S56: APT spectrum of $[\text{Zn}(\text{L}^3)]$ in CD_2Cl_2 at ambient temperature.

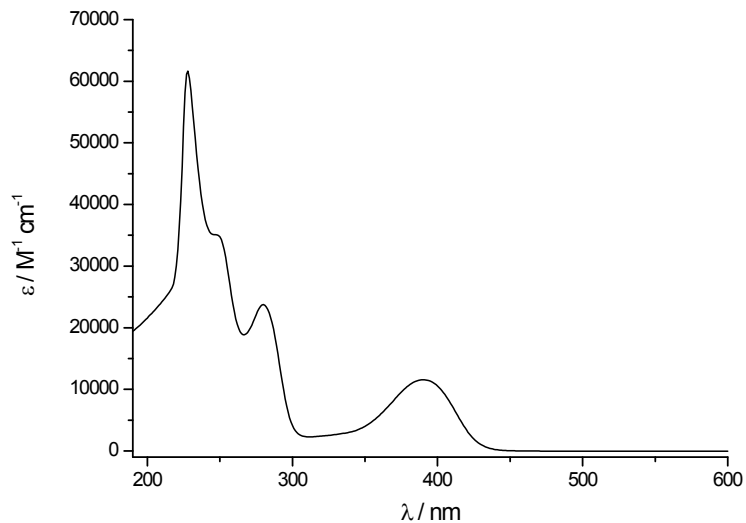


Figure S57. UV/Vis spectrum for **ZnL³** (MeCN, $[\text{ZnL}^3] = 2,5 \cdot 10^{-5} \text{ M}$)

11) Spectrophotometric titrations / Determination of Stability Constants

Batch data for $[Zn(L^1)]$

HypeSpec refinement output

Project title: Titration of H_2L^1 by $Zn(OAc)_2$
 Converged in 1 iterations with sigma = 0,021813

Log beta	value	standard deviation
AB	8.1672	0.4746

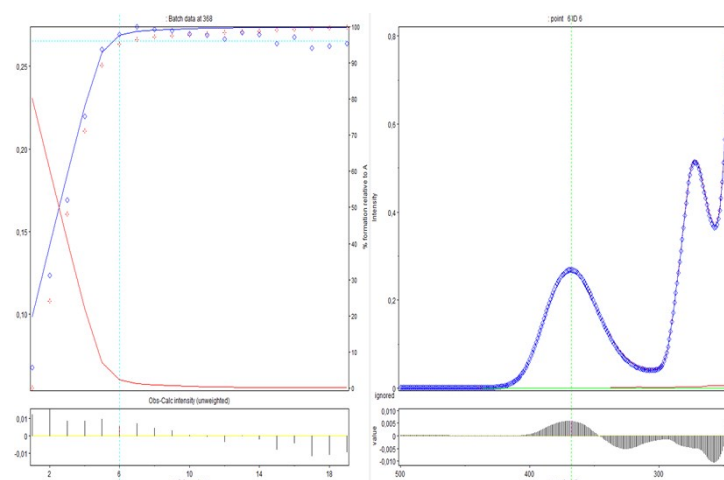


Figure S58: Titration isotherm extracted at 368 nm (left panel), spectrum corresponding to the 6th data point (right panel), and plot of residuals (bottom panels). Observed absorbance values are plotted as blue diamonds and the calculated ones as red crosses. The solid lines in the right panel show the calculated contribution of H_2L^1 (red), $Zn(OAc)_2$ (green) and the 1:1 complex (blue) to the total absorbance.

Batch data for $[Zn(L^2)]$

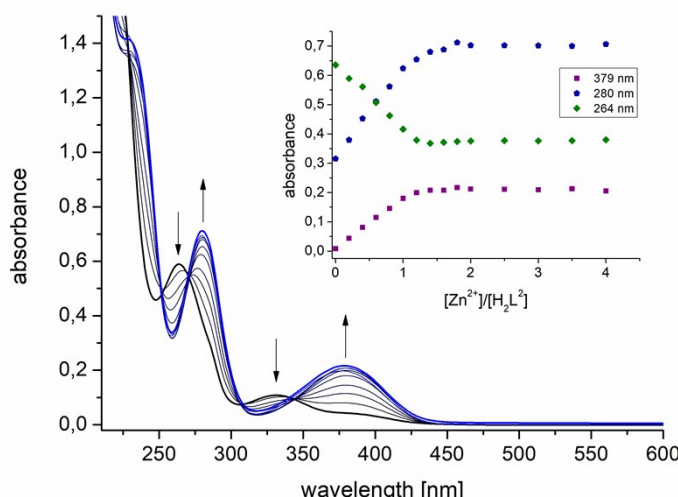


Figure S59: Spectrophotometric titration of H_2L^2 with Zn^{2+} in MeCN (10^{-2} M $N(nBu)_4PF_6$, $T = 298$ K). The inset shows the evolution of selected absorbance values versus the $[Zn^{2+}]/[H_2L^2]$ molar ratio.

HypeSpec refinement output

Project title: Titration of H_2L^2 by $\text{Zn}(\text{OAc})_2$
 Converged in 1 iterations with sigma = 6,9571E-03

	standard
Log beta	value
AB	5.6937
	0.0163

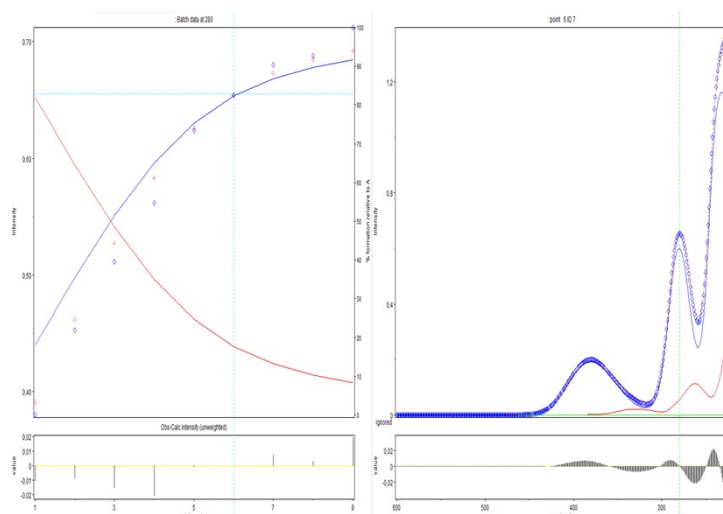


Figure S60: Titration isotherm extracted at 280 nm (left panel), spectrum corresponding to the 6th data point (right panel), and plot of residuals (bottom panels). Observed absorbance values are plotted as blue diamonds and the calculated ones as red crosses. The solid lines in the right panel show the calculated contribution of H_2L^2 (red), $\text{Zn}(\text{OAc})_2$ (green) and the 1:1 complex (blue) to the total absorbance.

Batch data for $[\text{Zn}(\text{L}^3)]$

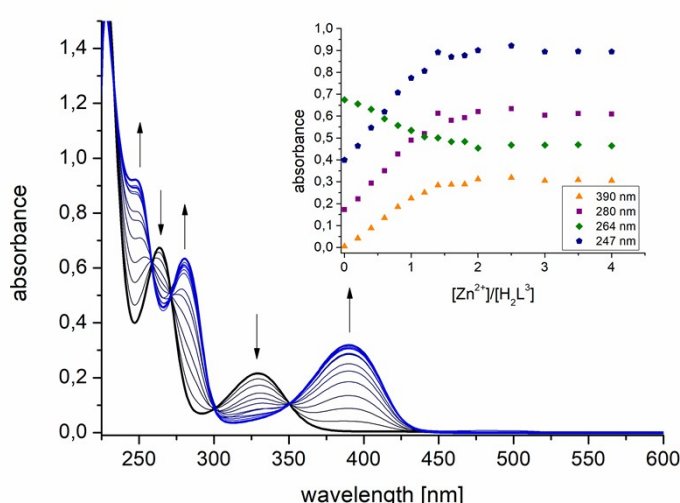


Figure S61: Spectrophotometric titration of H_2L^3 with Zn^{2+} in MeCN (10^{-2} M $\text{N}(n\text{Bu})_4\text{PF}_6$, $T = 298$ K). The inset shows the evolution of selected absorbance values versus the $[\text{Zn}^{2+}]/[\text{H}_2\text{L}^3]$ molar ratio.

HypeSpec refinement output

Project title: Titration of H_2L^3 by $\text{Zn}(\text{OAc})_2$
 Converged in 1 iterations with sigma = 0,011439

Log beta	value	standard deviation
AB	5.4629	0.0104

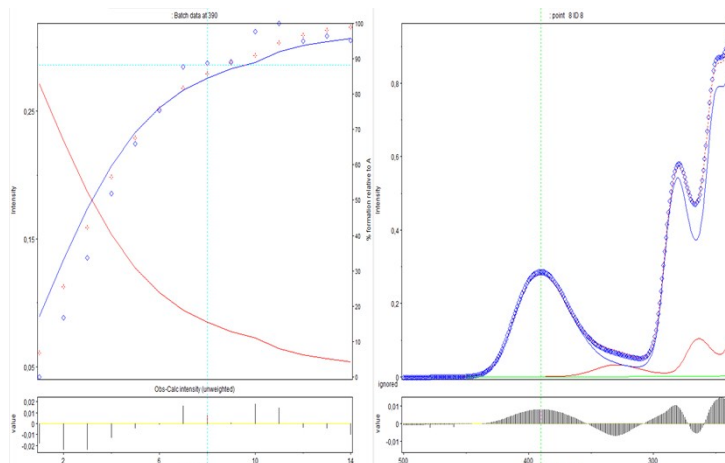


Figure S62: Titration isotherm extracted at 390 nm (left panel), spectrum corresponding to the 8th data point (right panel), and plot of residuals (bottom panels). Observed absorbance values are plotted as blue diamonds and the calculated ones as red crosses. The solid lines in the right panel show the calculated contribution of H_2L^3 (red), $\text{Zn}(\text{OAc})_2$ (green) and the 1:1 complex (blue) to the total absorbance.

Batch data for $[\text{Zn}(\text{L}^4)]$

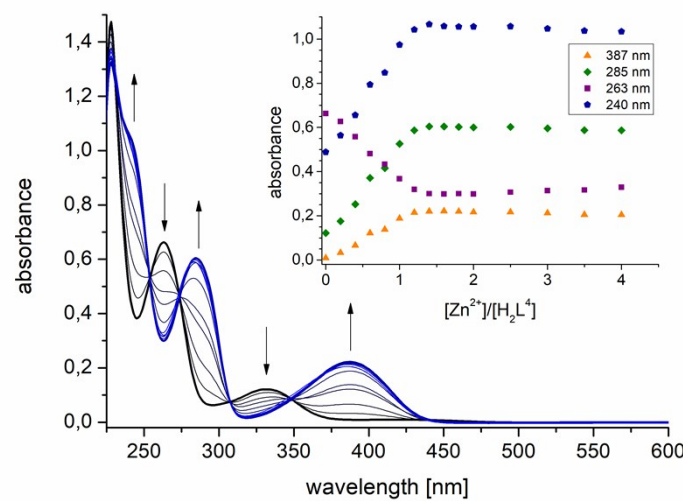


Figure S63. Spectrophotometric titration of H_2L^4 with Zn^{2+} in MeCN (10^{-2} M $\text{N}(n\text{Bu})_4\text{PF}_6$, $T = 298$ K). The inset shows the evolution of selected absorbance values versus the $[\text{Zn}^{2+}]/[\text{H}_2\text{L}^4]$ molar ratio.

HypeSpec refinement output

Project title: Titration of H_2L^4 by $\text{Zn}(\text{OAc})_2$
 Converged in 1 iterations with sigma = 0,011147

		standard
Log beta	value	deviation
AB	6.2775	0.0248

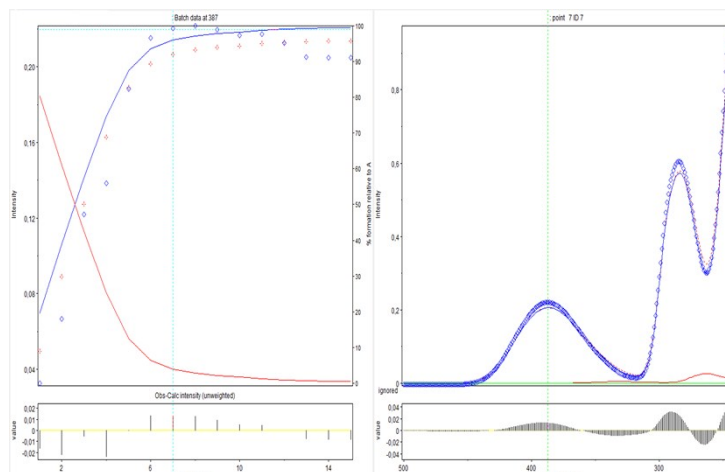


Figure S64: Titration isotherm extracted at 387 nm (left panel), spectrum corresponding to the 7th data point (right panel), and plot of residuals (bottom panels). Observed absorbance values are plotted as blue diamonds and the calculated ones as red crosses. The solid lines in the right panel show the calculated contribution of H_2L^4 (red), $\text{Zn}(\text{OAc})_2$ (green) and the 1:1 complex (blue) to the total absorbance.

Table S1. Cartesian Coordinates of $[Zn(L^{1'})_2]$ (PBE0, RIJCOSX, TZVP, TZV/J, ZORA).

C	0.09743537197142	0.08437607848630	0.14308490573337
C	-0.02145818984018	0.07712918124506	1.51334107752576
C	1.10830500680273	0.03301844532929	2.36408282076087
C	2.39333926443743	-0.01400781307382	1.73761991471572
C	2.47495222370125	-0.00774768900152	0.32955817830426
C	1.35614421279164	0.04231285472764	-0.46967714146590
H	-0.79877653462320	0.12157511346746	-0.46797985442712
H	-0.99699642929653	0.11061230780493	1.98662348263128
H	3.46062071868546	-0.04767096167963	-0.12599176713822
H	1.44658717930009	0.04753803287210	-1.54943809739002
C	3.64653079694521	-0.09726116713677	2.44217828754945
O	0.91415764987212	0.03178886151360	3.64816451509507
C	5.19554492466705	-0.22635459011380	4.21486059071427
H	4.52813587282411	-0.16973437043356	1.79704354013421
H	5.26512503001425	-1.09052731068933	4.87928424514679
H	5.91773478892131	-0.34318486788345	3.40255912906112
H	5.45526355817603	0.65981206071701	4.79997518027004
Zn	2.31170323174362	0.01195887143246	4.99040532036461
O	2.27842354496070	-1.39209627853418	6.32550378634124
N	2.23471733128951	1.53382618638423	6.27684073163920
N	3.83911229579680	-0.10509300641854	3.71337698313406
C	2.23426777539021	1.33481517523657	7.54700322191597
C	2.28261178207870	0.07610519480871	8.24479263818944
C	2.29386133966795	-1.20601130273329	7.61063138554593
H	2.18640574392667	2.21490891065055	8.19652759989175
C	2.31769412487455	-2.34170352369566	8.45425182591748
H	2.35497327558035	-3.13159736834817	10.43082841426597
H	2.32573496225002	-3.31496450113629	7.97517941132918
C	2.32318696866623	-0.97557755882221	10.44557393306607
C	2.33416565064280	-2.23120544039179	9.82510373349097
H	2.33421588714652	-0.89192568702493	11.52583905263911
C	2.29546272284261	0.14897022361028	9.65330689060473
H	2.28228899398100	1.13252422350960	10.11497523768021
C	2.15504987421661	2.89428594560991	5.78010645539905
H	2.06931500171841	3.61802918442814	6.59492694396041
H	3.04471735919427	3.12507556733605	5.18827050289882
H	1.28893268868227	2.99381901794704	5.12200492450485

Table S2. Cartesian Coordinates of $[Zn(L^{2'})_2]$ (PBE0, RIJCOSX, TZVP, TZV/J, ZORA).

C	-0.06019101570315	-0.36217107499400	0.17795938569293
C	-0.00313735898447	-0.29553410804881	1.55141004648321
C	1.23096109546979	-0.10277509782658	2.24129755956508
C	2.41455884495554	-0.09758703235544	1.44241465083300
C	2.31693033638171	-0.17632310840272	0.03741871200959
C	1.10416310426447	-0.28796500019774	-0.59772756742833
H	-1.03035607343325	-0.48859080848170	-0.29261097807436
H	3.23404677986815	-0.15835777746375	-0.54361542291485
H	1.04526875426485	-0.34081238367140	-1.67833730073185
C	3.75185862610034	-0.06798553630754	1.97449903740061
O	1.20377446633034	0.04254474629354	3.52783795065996
C	5.52603504762916	-0.09142487803924	3.52818259300044
H	4.54182325430364	-0.14871061493882	1.22146580593874
H	5.68309274110417	-0.91355338093860	4.22979722516416
H	6.13282181111871	-0.26725321305343	2.63601025900398
H	5.86036162402375	0.82733492477518	4.01698492409532

Zn	2.76941134326307	0.14407023238132	4.66090650922387
O	2.91408244968257	-1.26130062849833	5.97460916653006
N	2.74113710633465	1.64731705899779	5.96124392468355
N	4.11376598562852	0.00058708467277	3.20626479166657
C	2.73466189322996	1.43160572990820	7.22923901667733
C	2.75882419927022	0.16448340846117	7.91456496041895
C	2.82205653527441	-1.09853781587730	7.25375763961814
H	2.69036327578663	2.30433174772803	7.88833629180249
C	2.78343355998027	-2.26172591532654	8.07749606779857
H	2.73573648890700	-3.09066503224668	10.02628449803538
C	2.72734982855942	-0.92578036020842	10.08880215820258
C	2.74779855570334	-2.17167342846217	9.44910540926423
H	2.70373915887498	-0.86963910760270	11.17051647072201
C	2.72627427231599	0.21649263601263	9.32430178023793
H	2.69208305604474	1.19036792807382	9.80377050190951
C	2.67052370267389	3.01370008272972	5.47993601037043
H	2.61382265285847	3.73061542054762	6.30306803659933
H	3.54916314692393	3.23700753358973	4.86959289076283
H	1.79070637967620	3.13137176798531	4.84279643379399
O	2.86032700162081	-3.49679919216595	7.48734609046819
O	-1.16792228138464	-0.36318586351819	2.27335814253268
C	1.71571272499777	-3.85300526248463	6.71192527531887
H	0.83990787857351	-3.96448399902926	7.35883385838678
H	1.51864648810551	-3.10699049078788	5.94059859015798
H	1.94349354069282	-4.8085511081110	6.23991758360465
C	-1.27030198320155	-1.53472130484501	3.08351764188428
H	-1.21996263109249	-2.43162297152077	2.45772138715827
H	-2.23946397813524	-1.48987744490342	3.57989508648297
H	-0.47773838885847	-1.55943635914874	3.83363190498992

Table S3. Cartesian Coordinates of [Zn(L^{3'})₂] (PBE0, RIJCOSX, TZVP, TZV/J, ZORA).

C	4.54235898166334	0.75383681003833	-1.47504620064954
C	3.16937647372848	0.69206072987643	-1.55745524971914
C	2.42966554291903	0.02060527298768	-0.54463525733901
C	3.15606657893891	-0.60643175110456	0.51096210489000
C	4.56570109664846	-0.51394774359553	0.53516275279607
C	5.27575595084775	0.17066476769567	-0.42686972339440
H	5.08301470808847	1.28840975850138	-2.25270635944234
H	5.09317672489421	-0.99704582270209	1.35464241159854
C	2.54757389836279	-1.36465493367211	1.57250383852460
O	1.13856065166982	0.00991975984708	-0.64204622718863
C	0.90465462014430	-2.34759183628615	2.95659669340375
H	3.25540644179035	-1.87773515529289	2.23206950990380
H	0.25436163876549	-3.15149590865875	2.60385452418638
H	1.77184584943698	-2.78618831058904	3.45823222165613
H	0.33548693253060	-1.75681105745314	3.67915529319348
Zn	-0.07188259156248	-0.54415815401110	0.76339930219519
O	-1.65614783500512	-1.35807065465617	0.01822695787380
N	-0.99552811266034	1.01994929722993	1.59634210187795
N	1.29339510270179	-1.50963134145573	1.83564821273928
C	-2.18833220507094	1.32334091870034	1.22747490110382
C	-3.03853841144400	0.60194341934377	0.31419048603833
C	-2.74975287598230	-0.68963464340850	-0.21806114120290
H	-2.62638544854987	2.23960479852420	1.63634411194545
C	-3.73700520637268	-1.29407524157822	-1.04450998662454
H	-5.60731762838443	-1.07665366124705	-2.02646490471524
C	-5.14920644958206	0.70490948650262	-0.91668266718016
C	-4.87993488700083	-0.59461826303962	-1.37737369160733
C	-4.23372109742773	1.25714574424682	-0.04883838109144
H	-4.41777604517005	2.24275236553893	0.37166202659604
C	-0.28844104720483	1.90777105450863	2.49847804594056

H	-0.95027334439230	2.66456038962109	2.92896831140806
H	0.16473524220760	1.32961854396279	3.30645018933375
H	0.51779611527246	2.40973152857352	1.95572418468130
C	-3.49555533486217	-2.68951511936237	-1.53016877081154
H	-2.61830914186529	-2.74234155770977	-2.18201136483661
H	-3.29537780540026	-3.36517842807670	-0.69405199844504
H	-4.35884769158559	-3.06280301347262	-2.08411501016146
C	2.41125073479233	1.33022899037533	-2.67681894572708
H	1.82675925681320	0.58964815350374	-3.23209550693821
H	1.69257413351998	2.06115035226227	-2.29435989659413
H	3.08648608004145	1.83249847485034	-3.37199461006473
C	6.77351910098386	0.28902264335593	-0.39750183612455
H	7.14231384068924	0.50407365111610	0.60826367280800
H	7.26047295294997	-0.63111380340908	-0.73778516398648
H	7.11070420511381	1.09177133590818	-1.05568960749692
C	-6.37366389354443	1.45093093025565	-1.36813961795798
H	-6.81188408344131	2.03411827641252	-0.55427413744501
H	-6.13515756834092	2.15272337625970	-2.17380644791710
H	-7.13584915066474	0.76809657078222	-1.74862115003279